Performance Enhancement of Scalable Cell-free Massive MIMO Systems Using Dynamic Cooperation Cluster Optimization Concept

Tadelech Amdemariam

A Research Thesis Submitted to the Department of Electronics and Communication Engineering, School of Electrical Engineering & Computing In Partial Fulfillment of the Requirements of the Degree of Master of Science in Communication Engineering

Office of Graduate Studies
Adama Science and Technology University

June, 2024

Adama, Ethiopia

Performance Enhancement of Scalable Cell-free Massive MIMO Systems Using Dynamic Cooperation Cluster Optimization Concept

Tadelech Amdemariam

Main Advisor: Dr. Ram Sewak Singh

Co Advisor: Mr. Eshetu Tesema

A Research Thesis Submitted to the

Department of Electronics and Communication Engineering

School of Electrical Engineering and Computing

Office of Graduate Studies

Adama Science and Technology University

June, 2024

Adama, Ethiopia.

DECLARATION

I declare that this research thesis entitled "**Performance Enhancement of Scalable Cell-free Massive MIMO Systems Using Dynamic Cooperation Cluster Optimization Concept**,'' own work and has not been submitted to any university for similar purpose. The references used in this research thesis are duly recognized by formatting citation.

_________________	_______________	___________
Name of student	Signature	Date

RECOMMENDATION OF ADVISORS

We, the main advisor and co-advisor for this research thesis, attest that we have provided the student with close guidance throughout the research thesis's development. We have also reviewed the draft thesis research thesis, "**Performance Enhancement of Scalable Cell-free Massive MIMO Systems Using Dynamic Cooperation Cluster Optimization Concept**," which was prepared by Tadelech Amdemariam with our assistance. As a result, we advise sending the research thesis to the department for additional examination and assessment.

___________________	________________	________________
Major Advisor	Signature	Date
________________	_________________	________________
Co-advisor	Signature	Date

APPROVAL PAGE FOR RESEARCH THESIS

We hereby attest that the completed research thesis, "**Performance Enhancement of Scalable Cell-free Massive MIMO Systems using Dynamic Cooperation Cluster Optimization Concept**" adequately incorporates the advice and suggestions provided by the research thesis review committee. Written by Tadelech Amdemariam

________________	________________	________________
Main Advisor	Signature	Date
________________	________________	________________
Co-Advisor	Signature	Date

APPROVAL OF BOARD OF REVIEWERS

The research thesis titled "**Performance Enhancement of Scalable cell-free Massive MIMO Systems Using dynamic cooperation cluster optimization concept** "was read and evaluated by us, the undersigned members of the Board of Reviewers for Tadelech Amdemariam open defense. We also evaluated the candidate's comprehension of the research thesis. Thus, this certifies that the thesis proposal is approved and that we advise putting it into practice.

________________	________________	________________
Chairperson	Signature	Date
________________	________________	________________
External Examiner	Signature	Date
________________	________________	________________
Internal Examiner	Signature	Date

Final approval and acceptance of the research thesis is contingent upon submission of its final copy to the Office of Postgraduate Studies through the Department Graduate Council and School Graduate Committee.

________________	________________	________________
Department Head	Signature	Date
________________	________________	________________
School Dean	Signature	Date
________________	________________	________________
Postgraduate Dean	Signature	Date

ACKNOWLEDGMENT

First of all, I would like to thank the almighty GOD for helping me in the successful accomplishment of this research thesis. Next, my deep gratitude goes to my advisor Ram Sewak Singh and Eshetu Tesema for their constructive comments and suggestions to develop this research thesis. In addition, my heart-felt gratitude and appreciation for the people who made contributions to make this research thesis possible.

Last but not least I would like to thank my brother, sister, friends and my husband who supported me in all aspects.

TABLE OF CONTENTS

DECLARATION i
RECOMMENDATION OF ADVISORS ii
APPROVAL PAGE FOR RESEARCH THESIS iii
APPROVAL OF BOARD OF REVIEWERS iv
ACKNOWLEDGMENT v
TABLE OF CONTENTS vi
LIST OF FIGURES x
ABBREVIATIONS xii
ABSTRACT xiii
1. INTRODUCTION 1
1.1. Background 1
1.2. Statement of the Problem 2
1.3. Objective 3
1.3.1. General objective 3
1.3.2. Specific objectives 3
1.4. Significance of the Study 3
1.5. Expected Outcomes of the Study 5
1.6. Scope and Limitations of the Study 5
2. LITERATURE REVIEW 7
2.1. Introduction 7
2.2. Spectral Efficiency of Cell-free Massive MIMO Systems 9
2.4. Related Works 9
3. METHODOLOGY 14
3.1. Material 14
3.2. Methods of the Study 14
3.2.1. Simulation Methods 14
3.4. SE of Centralized cell-free Downlink Data Transmission 17
3.4.1. MMSE precoding 19
3.4.2. PMMSE precoding 19
3.4.3. PRZF precoding 20

3.5. Downlink Operation in a Distributed System...20
3.6. Spectral Efficiency in a Distributed Downlink Operation.....................................21
3.6.1. LMMSE precoding..22
3.6.2. LPMMSE precoding..22
3.7. Dynamic Clustering of Cooperation (DCC)..22
3.8. Proposed Method...23
3.9. Block Diagram of Proposed Method..26
4. Results and Discussions..27
4.1. Performance comparrision of Scalable precoding with the Existing precoding 28
4.1.1. Performance comparrision of Scalable precoding with the Scalable precoding based on Average Spectral efficiency..28
4.1.2. Performance comparrision of proposed precoding scheme with Scalable precoding based on Sum SE 36
4.1.3. Performance comparrision of Scalable precoding with the Existing precoding based on CDF and Spectral efficiency..42
4.1.4. Performance comparision of Proposed Method (Precoding) with Scalable precoding based on BER and SNR valus. 49
5. CONCLUSION AND RECOMMENDATION..56
5.1. Conclusion..56
5.2. Recommendation..57
REFERENCES 58

LIST OF TABLES

Table 2. 1: Summary of some related literature 10

Table 4. 1: Simulation Parameters (Björnson & Sanguinetti, 2019b; Sheikh et al., 2023; Zhang et al., 2019; Zheng et al., 2022) 28

Table 4. 2: Average DL SE per UE with different scalable and proposed precoding schemes at L=400 and N=1 in a 1km^2 region.. 30

Table 4. 3: Average DL SE per UE with different scalable and proposed precoding schemes at L=400 and N=2 in a 1km^2 region. 32

Table 4. 4: Average DL SE per UE with different scalable and proposed precoding schemes at L=400 and N=3 in a 1km^2 region. 33

Table 4. 5: Average DL SE per UE with different scalable and proposed precoding schemes at L=400 and N=4 in a 1km^2 region. 35

Table 4. 6: Sum DL SE per UE with different scalable and proposed precoding schemes at L=400 and N=1 in a 1km^2 region for different number of UEs. 37

Table 4. 7: Sum DL SE per UE with different scalable and proposed precoding schemes at L=400 and N=2 in a 1km^2 region for different number of UEs. 38

Table 4. 8: Sum DL SE per UE with different scalable and proposed precoding schemes at L=400 and N=3 in a 1km^2 region for different number of UEs. 40

Table 4. 9: Sum DL SE per UE with different scalable and proposed precoding schemes at L=400 and N=4 in a 1km^2 region for different number of UEs. 41

Table 4. 10: DL SE per UEs for the proposed method and different scalable precoding schemes at L = 400, N = 1 and k=100 in a 1 km^2 area. 43

Table 4. 11: DL SE per UEs for the proposed method and different scalable precoding schemes at L = 400, N = 2 and k=100 in a 1 km^2 area. 45

Table 4. 12: DL SE per UEs for the proposed method and different scalable precoding schemes at L = 400, N = 3 and k=100 in a 1 km^2 area. 46

Table 4. 13: DL SE per UEs for the proposed method and different scalable precoding schemes at L = 400, N = 4 and k=100 in a 1 km^2 area. 48

Table 4. 14: BER of proposed method and other scalable precoding techniques at L = 400 and N = 1, and K=100 with different SNR values. 50
Table 4. 15: BER of proposed method and other scalable precoding techniques at L = 400 and N = 2, and K=100 with different SNR values. 52
Table 4. 16: BER of proposed method and other scalable precoding techniques at L = 400 and N = 3, and K=100 with different SNR values. 53
Table 4. 17: BER of proposed method and other scalable precoding techniques at L = 400 and N = 4, and K=100 with different SNR values. 55

LIST OF FIGURES

Figure 3. 1. Flow chart of proposed system 15
Figure 3. 2. Block Diagram of Scalable cell free Massive Network(Björnson & Sanguinetti, 2020) 16
Figure 3. 3: Indicates a dynamic clustering cooperation involving a large number of access points and three UEs(Demir et al., 2021; Interdonato et al., 2019). 23
Figure 3. 4. Block diagram of proposed based on Dynamic Cooperation Cluster Optimization concept 26

Figure 4. 1. Average DL SE per UE with different scalable and proposed precoding schemes at L=400 and N=1 in a 1km^2 region. 29
Figure 4. 2. Average DL SE per UE with different scalable and proposed precoding schemes at L=400 and N=2 in a 1km^2 region. 31
Figure 4. 3. Average DL SE per UE with different scalable and proposed precoding schemes at L=400 and N=3 in a 1km^2 region. 33
Figure 4. 4. Average DL SE per UE with different scalable and proposed precoding schemes at L=400 and N=4 in a 1km^2 region. 34
Figure 4. 5. Sum DL SE per UE with different scalable and proposed precoding schemes at L=400 and N=1 in a 1km^2 region. 36
Figure 4. 6. Sum DL SE per UE with different scalable and proposed precoding schemes at L=400 and N=2 in a 1km^2 region for different number of UEs. 38
Figure 4. 7. Sum DL SE per UE with different scalable and proposed precoding schemes at L=400 and N=3 in a 1km^2 region for different number of UEs. 39
Figure 4. 8. Sum DL SE per UE with different scalable and proposed precoding schemes at L=400 and N=4 in a 1km^2 region for different number of UEs. 41
Figure 4. 9. DL SE per UEs for the proposed method and different scalable precoding schemes at L = 400, N = 1 and k=100 in a 1 km^2 area. 43
Figure 4. 10. DL SE per UEs for the proposed method and different scalable precoding schemes at L = 400, N = 2 and k=100 in a 1 km^2 area. 44
Figure 4. 11. DL SE per UEs for the proposed method and different scalable precoding schemes at L = 400, N = 3 and k=100 in a 1 km^2 area. 46

Figure 4. 12. DL SE per UEs for the proposed method and different scalable precoding schemes at L = 400, N = 4 and k=100 in a 1 km^2 area. 47
Figure 4. 13. BER of proposed method and other scalable precoding techniques at L = 400 and N = 1, and K=100 with different SNR values. 50
Figure 4. 14. BER of proposed method and other scalable precoding techniques at L = 400 and N = 2, and K=100 with different SNR values. 51
Figure 4. 15. BER of proposed method and other scalable precoding techniques at L = 400 and N = 3, and K=100 with different SNR values. 53
Figure 4. 16. BER of proposed method and other scalable precoding techniques at L = 400 and N = 4, and K=100 with different SNR values. 54

ABBREVIATIONS

APs	Access points
BER	Bit Error Rate
CPU	Central processing center
CSI	Channel state information
DCC	Dynamic Clustering Cooperation
DL	Down Link
5G	Fifth generations
GD	Gradient Descent
GHz	Giga Hertz
IoT	Internet of Things
KHz	Kilo Hertz
Km	Kilo Meter
MIMO	Multiple-Input Multiple-Output
mMIMO	Massive multiple-input multiple-output
MMSE	Minimum Mean Square Error
MSE	Mean Square Error
mW	Milli Watt
LMMSE	Linear Minimum Mean Square Error
PMMSE	Partial Minimum Mean Square Error
PLMMSE	Partial Linear Minimum Mean Square Error
PRZF	Partial Regularized Zero Forcing
QAM	Quadrature Amplitude Modulation
RZF	Regularized Zero Forcing
SE	Spectral Efficiency
SNR	Signal to Noise Ratio
UL	Uplink
ZF	Zero Forcing

ABSTRACT

Downlink cell-free massive MIMO is an emerging wireless communication system that aims to overcome the limitations of traditional cellular networks. In contrast, a cell-free massive MIMO network uses a large number of distributed access points (APs) or remote radio heads to provide coverage, without the concept of distinct cells. This allows for more uniform signal coverage and helps eliminate cell-edge problems. However, the difficulty lies in realizing the benefits of cell-free operation in a practical manner. These challenges are Efficient coordination, channel Estimation, Scalability, Hardware complexity and so on. In response to this challenge, this thesis presents a dynamic cooperation cluster concept for scalable Cell-Free Massive MIMO systems. Leveraging the dynamic cooperation cluster concept, the Gradient Descent based Minimum Mean Square Error approach introduces an algorithm for joint initial access, and cluster formation that has been rigorously proven to be scalable. The gradient descent optimization technique is employed to progressively refine the MMSE precoding matrix. Additionally, it adopts precoding techniques to ensure scalability. Furtherly enhances the spectral efficiency, signal-to-interference-plus-noise ratio and bit error rate (BER) compared with Partial MMSE (Minimum mean square Error), LMMSE (Linear minimum mean square Error), RZF (Regularized Zero Forcing) precoding. The performance gap between the proposed method and the other techniques increases as the SNR, N, and number of UEs increases. This implies that the proposed method is particularly effective in scenarios with high SNR, number of UEs. This is achieved by calculating the gradient of the mean squared error (MSE) with respect to the precoding matrix PMMSE, and then using this gradient information to iteratively update the precoding matrix. The goal of this approach is to minimize the MSE between the intended signal and the received signal, and improves the performance of desired system.

***Keyword**s: Scalability Cell-Free, Cluster formation, Gradient Descent, PMMSE, PLMMSE, PRZF, precoding.*

CHAPTER ONE

1. INTRODUCTION

1.1. Background

The utilization of a substantial number of antennas at base station along with beamforming technology, enables massive multiple-input multiple-output (mMIMO) technology to deliver services to multiple users simultaneously within same time frequency resources (Ding et al., 2020). By implementing this technology, not only does the capacity of the conventional cellular network experience significant enhancement, but it also facilitates the gradual transition of fifth-generation (5G) communication from a mere theoretical concept to practical implementation (Marzetta et al., 2020). Nevertheless, as researchers delve deeper into the study of mMIMO technology, they have discovered that the existing cell mode within traditional cellular networks exposes edge users to heightened susceptibility to severe inter-cell interference, resulting in a substantial impact on the quality of service they receive (Ding et al., 2020). The concept of the cell-free massive MIMO has the potential to greatly reduce interference of cellular networks (Interdonato et al., 2023). Since cell-free frameworks have a large coverage area, they are inherently equipped with diversity gains, thus providing immunity against fading and shadowing effects (H. Zhang et al., 2022). Nonetheless, the cell-free framework necessitates a significant volume of control signaling with the core network and amplified backhaul demands. The fundamental characteristic of cell-free entails establishing a network environment in which all access points (APs) collaborate to collectively cater to user equipment (UEs) and eradicate any inter-cell interference (Garg et al., 2022). The effectiveness of the cell-free framework hinges on obtaining precise statistical data regarding the channel state information (CSI) (Zaher et al., 2022). The estimation of these CSI values is essential for implementing precoding during transmission and reducing interference in the spatial domain. However, obtaining these estimates involves the transmission and reception of pilot signals, which in turn leads to increased overhead and computational complexity (Ruan et al., 2022).

This research aims to enhance the performance of scalable cell-free massive MIMO systems using the dynamic cooperation cluster optimization concept. By addressing the challenges of scalability, interference management, and resource allocation, the research seeks to unlock the full potential of cell-free massive MIMO systems and provide seamless connectivity to a massive number of users.

The centralized architecture of cell-free massive MIMO is well-suited for QAM, as the central unit can perform efficient QAM demodulation and detection, leveraging advanced algorithms like maximum-likelihood detection. QAM modulation can effectively leverage the spatial multiplexing capabilities of massive MIMO in cell-free systems, leading to significant improvements in spectral efficiency and data rates. While QAM is a suitable choice, the specific modulation order and the trade-offs between spectral efficiency and robustness need to be carefully considered in the design of cell-free massive MIMO systems, based on factors like channel conditions, user distribution, and system requirements (Hoffmann & Kryszkiewicz, 2024; Nguyen et al., 2020; Özdogan et al., 2019).

1.2. Statement of the Problem

The research on the performance enhancement of scalable cell-free Massive MIMO systems using the dynamic cooperation cluster optimization concept aims to address several key problems associated with these systems. Cell-free massive MIMO systems have emerged as a promising technology for future wireless communication networks. These systems utilize a large number of distributed access points (APs) to serve multiple users simultaneously, leading to improved spectral efficiency, increased capacity, and enhanced coverage. However, despite their potential, cell-free massive MIMO systems face several challenges that hinder their performance and scalability. This research aims to address these challenges and propose a dynamic cooperation cluster optimization concept with Gradient Descent based optimizer to enhance the performance of scalable cell-free massive MIMO systems and the following are the key problems in the field of wireless communication networks:

1. Inter-Cluster Interference: In cell-free Massive MIMO systems the lack of coordination among APs can lead to interference between different cooperation clusters, degrading the system performance and limiting the achievable throughput. Efficient management of inter-cluster interference is crucial to improve the overall system capacity and enhance the user experience.

2. Resource Allocation Optimization: The dynamic nature of wireless environments and varying channel conditions demand adaptive allocation of resources such as transmit power, time slots, and frequency bands. Optimal resource allocation strategies are needed to ensure efficient utilization of available resources, minimize interference, and improve the system's spectral efficiency and capacity.

3. Scalability Challenges: As the number of APs and users increases, the signaling overhead and computational complexity associated with cooperation cluster formation and management become significant. The successful implementation of cell-free Massive MIMO systems heavily relies on the development of scalable algorithms and strategies capable of effectively managing a substantial number of access points (APs) and users. It is crucial to maintain performance levels and minimize unnecessary overhead in order to achieve this goal. Therefore, the research aims to address these problems and propose innovative solutions to enhance the performance, scalability, and energy efficiency of scalable cell-free Massive MIMO systems. By developing dynamic cooperation cluster optimization concepts, efficient resource allocation algorithms, and scalable strategies, the study aims to overcome these challenges and improve system capacity, spectral efficiency, and user experience in wireless communication networks. Ultimately, the research findings will contribute to the advancement of cell-free Massive MIMO technology and pave the way for more efficient and reliable wireless communication systems in the future.

1.3. Objective

1.3.1. General objective

The primary aim of this research is to improve the performance of scalable cell-free massive MIMO systems in next-generation wireless communication by employing the concept of dynamic cooperation cluster optimization.

1.3.2. Specific objectives

- Investigate the impact of dynamic cooperation cluster optimization on the performance of scalable cell-free Massive MIMO systems.
- Optimized the precoding vector and MSE of PMMSE precoding technique using gradient Descent based optimizer.
- Analyze the BER and Spectral efficiency in scalable cell-free Massive MIMO systems for different number of antennas and UEs.
- To compare the performance of Gradient Descent based PMMSE precoding, LPMMSE and PRZF precoding techniques based on sum SE, average SE, BER and SNR values.

1.4. Significance of the Study

The research on the performance enhancement of scalable cell-free massive MIMO systems using the dynamic cooperation cluster optimization concept holds significant importance in the field of wireless communication systems. The following points highlight the significance of this research:

- **Improved Spectral Efficiency:** Comparing cell-free Massive MIMO systems to conventional cellular networks, a considerable increase in spectral efficiency could be achieved. Through dynamic optimization of the collaboration clusters, this study seeks to improve these systems' spectral efficiency even more. By reducing inter-cluster interference and optimizing resource allocation, the suggested approach will boost overall system capacity and data rates. The results of this study will help wireless networks satisfy the growing demand for high-speed data transmission while making the most use of the spectrum that is available.

- **Improved System Efficiency:** Effective resource allocation and interference control are critical components of cell-free Massive MIMO systems performance. The goal of this research is to enhance the system performance in terms of coverage, quality of service, and reliability by creating a dynamic cooperation cluster optimization approach. Strong and dependable communication will be ensured by the suggested algorithms and methods, which will adaptively distribute resources based on changing channel conditions and user requirements. The implementation of more dependable and effective wireless communication networks will be made possible by the study's conclusions.
- **Scalability and Flexibility:** The practical implementation of cell-free Massive MIMO systems depends heavily on scalability. As the number of access points rises, existing systems become more difficult computationally and in terms of signaling overhead. This research attempts to solve these restrictions by presenting scalable algorithms for cooperative cluster development and management. The established paradigm will allow the system to accommodate more users while lowering overhead and preserving effective resource allocation. The results of this research will help cell-free Massive MIMO systems become more flexible and scalable, which will enable practical use in real-world scenarios.
- **Energy Efficiency:** With the growing concern for environmental sustainability, wireless communication systems must make efficient use of energy resources. In addition to focusing on energy efficiency, the suggested dynamic cooperation cluster optimization model will also minimize needless interference and optimize resource allocation. This research can aid in the creation of sustainable and environmentally friendly wireless communication networks by lowering energy consumption.
- **Future Technology Advancements**: The study of how to use the dynamic cooperation cluster optimization concept to improve the performance of scalable cell-free Massive MIMO systems is in line with the ideas and developments that will shape wireless communication networks in the future. The results of this

investigation will offer significant perspectives and recommendations for the development and execution of next-generation wireless networks. The suggested ideas and algorithms can be used as a starting point for additional study and advancement in the area, opening the door to more sophisticated and effective wireless communication systems.

The significance of this study lies in its potential to improve the performance, spectral efficiency, scalability, and energy efficiency of cell-free Massive MIMO systems. This work is important because it can lead to better cell-free Massive MIMO system performance, spectrum efficiency, scalability, and energy efficiency. This research advances wireless communication networks by tackling the problems encountered by current systems and putting forward creative alternatives.

1.5. Expected Outcomes of the Study

After the accomplishment of the thesis, the expected outcome of the study on the performance enhancement of scalable cell-free Massive MIMO systems using the dynamic cooperation cluster optimization concept is the development of innovative solutions that significantly improve the system's performance, scalability, and efficiency. By mitigating inter-cluster interference, optimizing resource allocation, and proposing scalable algorithms for cooperation cluster formation and management, the study aims to achieve enhanced spectral efficiency, increased system capacity, and improved overall user experience in wireless communication networks. The expected outcome will contribute to the advancement of cell-free Massive MIMO systems, enabling their successful deployment in future wireless communication networks and paving the way for more efficient and reliable wireless technologies.

1.6. Scope and Limitations of the Study

The scope of the study on the performance enhancement of scalable cell-free Massive MIMO systems using the dynamic cooperation cluster optimization concept is focused on improving the performance and scalability of these systems. The study will involve the development and evaluation of algorithms, strategies, and concepts related to dynamic cooperation cluster optimization and resource allocation. It will consider aspects such as inter-cluster interference mitigation, resource allocation optimization, scalability, and energy efficiency. The research will be applicable to various wireless communication scenarios, including urban environments, indoor deployments, and outdoor networks. Mathematical modeling, simulations, and possibly experimental evaluations will be used to validate the proposed concepts and algorithms. The study on the performance enhancement of scalable cell-free Massive MIMO systems using the dynamic cooperation cluster optimization concept has certain limitations. Firstly, the research is likely to rely on simulation-based evaluations, which may not fully capture real-world deployment challenges and variations. Additionally, the study may make simplifying assumptions regarding system models, channel conditions, and user behaviors, which may not precisely represent the complexities of real-world systems. Resource constraints, such as time, funding, and computational resources, may also limit the extent of exploration of system configurations and scenarios. Furthermore, the practical implementation of the developed concepts and algorithms may pose challenges related to hardware limitations, protocol compatibility, and system integration. Despite these limitations, the study will provide valuable insights into enhancing the performance of scalable cell-free Massive MIMO systems and guide future research and development efforts in the field of wireless communication networks.

CHAPTER TWO

2. LITERATURE REVIEW

2.1. Introduction

In a cell-free network, where the number of users accessing the network is continuously increasing, an appropriate power control algorithm is necessary to address the scalability challenge. It is important to note that in this scenario, each access point (AP) makes independent power allocation decisions, without knowledge of the power allocation at neighboring APs. As a result, developing scalable solutions to this problem is quite challenging (Papazafeiropoulos et al., 2021). By transmitting a signal in a coordinated, phase-aligned manner from multiple antennas, the power received at the destination can be increased without needing to boost the total amount of power being transmitted (Zhang et al., 2024). The concept of beamforming, where signals from co-located antenna arrays are transmitted in a coordinated, phase-aligned manner to increase the received power, can also be applied when transmitting signals coherently from multiple, distributed Aps (Abdallah & Mansour, 2020). Even if the individual access points (APs) have varying channel conditions to a given receiver, the advantage of transmitting the signal coherently from multiple APs outweighs the benefit of only using the AP with the best channel. Transmitting the signal in a coordinated, phase-aligned manner from multiple distributed APs, rather than a single AP, is referred to by various names, such as "Network MIMO" (Interdonato et al., 2019). In cell-free massive MIMO systems, a large number of access points (APs), each equipped with one or more antennas, simultaneously provide service to all users by leveraging local channel state information (CSI) and performing coordinated, joint transmission (Rahmani et al., 2022). The access points (APs) transmit the uplink data received from users back to a central processing unit (CPU) over a backhaul link. The CPU then sends the downlink data and power control coefficients back to the APs. This backhaul link between the APs and CPU enables the CPU to use a centralized processing approach to efficiently allocate various network resources, greatly improving the quality of service experienced by the users (Björnson & Sanguinetti, 2019a). Cell-free massive MIMO technology is particularly well-suited for high-traffic, "hot-spot" locations such as railway stations, airports, stadiums, large shopping malls, and smart factories.

This suitability provides a promising direction for research into next-generation mobile communication network architectures (Sheela Rani et al., 2022). Studies have demonstrated that cell-free massive MIMO can significantly increase user data rates, several times higher compared to conventional small cell architectures, by employing matched filtering in the uplink and conjugate beamforming in the downlink. In addition to the high spectral efficiency achieved, cell-free massive MIMO can also play a crucial role in reducing the overall power consumption of the transmission system (Zheng et al., 2024).

The cell-free network architecture has developed from its earlier incarnations, such as network MIMO or coordinated multipoint implementations (Björnson & Sanguinetti, 2020). In network MIMO approaches, it was assumed that all the access points (APs) would have knowledge of the full channel state information (CSI) for the entire network, and would be able to share this information with all the users. However, this idealized form of a truly cell-free network, although theoretically preferred, was not practically feasible in reality. This is because it would have led to an enormous increase in the signaling overhead required for training and data transmission (Hassan et al., 2023).

The paper (Ngo et al., 2017) analyzes the overall energy efficiency of cell-free massive MIMO systems. Cell-free massive MIMO refers to a network architecture where numerous distributed access points (APs) simultaneously serve a smaller number of user devices (UEs) on the same time-frequency resources. The total energy efficiency is optimized by jointly tuning the number of active APs, the transmit power per AP, and the bandwidth allocation.

The paper (X. Zhang, T. Liang, et al., 2022) examines the secrecy performance of a reconfigurable intelligent surface (RIS)-assisted cell-free massive MIMO system that employs low-resolution analog-to-digital converters (ADCs) at the access points (APs). They analyzed the impact of various system parameters, such as the number of RIS elements, ADC resolution, and the number of AP antennas, on the secrecy performance. The results show that the secrecy performance can be significantly improved by increasing the number of RIS elements and the ADC resolution, but higher ADC resolution leads to increased power consumption.

In this paper (Zhang et al., 2019) the author introduces cell-free massive MIMO as a promising approach for future wireless communication systems beyond 5G. Cell-free massive MIMO is characterized by a network architecture with a large number of distributed access points (APs) jointly serving a much smaller number of user equipment (UEs). The paper demonstrates that cell-free massive MIMO can provide significant improvements over conventional cellular networks in terms of higher spectral efficiency, improved energy efficiency, enhanced coverage and connectivity, and greater robustness to interference and fading.

2.2. Spectral Efficiency of Cell-free Massive MIMO Systems

Cell-free massive MIMO systems have the potential to deliver significant SE improvement compared to traditional cellular networks, but the practical implementation requires addressing various technical challenges. Such techniques are listed in this section.

- **Favorable Propagation:** The channel vectors between the distributed access points (APs) and user equipment (UEs) are typically more orthogonal in cell-free networks. This helps reduce inter-user interference, enabling more efficient spatial multiplexing and higher spectral efficiency.
- **Macro-Diversity Gain:** Cell-free systems leverage the macro-diversity provided by the distributed APs. UEs can be served by multiple APs simultaneously, increasing the received signal power and improving spectral efficiency.

2.3. Energy Efficiency of Cell-free Massive MIMO System

(Björnson & Sanguinetti, 2019a) This paper provides a comprehensive analysis of the energy efficiency in cell-free massive MIMO systems. The authors derive analytical expressions for the energy efficiency and identify the key factors that influence it, such as the number of access points, transmit power, and hardware efficiency. They show that cell-free massive MIMO can achieve significantly higher energy efficiency compared to conventional cellular systems, especially in scenarios with a large number of access points.

(Xia et al., 2021) This paper presents a joint optimization framework for energy efficiency and spectral efficiency in cell-free massive MIMO systems. The authors derive analytical expressions for the energy efficiency and spectral efficiency, and then propose an optimization algorithm to find the Pareto-optimal trade-off between the two performance metrics. The results show that the proposed joint optimization can achieve a significant improvement in both energy efficiency and spectral efficiency compared to conventional approaches.

2.4. Related Works

The following literature review offers an overview of the current state of research on improving the performance of scalable cell-free massive MIMO systems using the dynamic cooperation cluster optimization concept, considering the research that has been done in this area recently. However, further research is still needed to fully characterize cell-free massive MIMO systems. For instance, the use of non-orthogonal downlink pilot signals should be explored as a means to increase the number of served user equipment’s (UEs). Additionally, more advanced power control algorithms would be desirable to enhance the overall performance of these systems.

Table 2. 1: Summary of some related literature

Authors/year	Tittle	Theoretical Model	Proposed-method	Findings	Research gap
(Papazafeiropoulos et al., 2021)	Scalable Cell-Free Massive MIMO Systems: Impact of Hardware Impairments	Obtain HA-PMMSE precoding to achieve higher SE by minimizing MSE	HA-based MMSE combining/precoding scheme to achieve high SE of scalable cell free massive MIMO system	Scalability, precoding optimization and enhanced downlink spectral efficiency	The HA receivers outperform those which are hardware unaware of the presence of both additive HWIs and PN. Furtherly optimize the precoding vector can minimize MSE, we can enhance the SE using gradient descent method
(Hassan et al., 2023)	On Scalability of FDD-Based Cell-Free Massive MIMO	FDD based scalable cell free massive system to obtain enhanced spectral efficiency energy efficiency	DCC method was implemented for angle-dependent MF, angle-dependent LP-MMSE, and angle-dependent MMSE	Employed the idea of dynamic cooperative clustering to calculate effective and scalable beamforming and combining vector formulations. The DCC method was	FDD-based systems exhibit greater computational complexity when compared to their TDD counterparts. Additionally, FDD-based systems lack channel reciprocity.

				implemented for angle-dependent MF, angle-dependent LP-MMSE, and angle-dependent MMSE formulations.	
(Zhang et al., 2019)	Cell-Free Massive MIMO: A New Next-Generation Paradigm	CF massive MIMO systems provide a better coverage than conventional collocated massive MIMO systems and uncoordinated small cells.	The analysis focuses on examining signal processing techniques used to reduce the burden on the fronthaul, specifically for joint channel estimation and transmit precoding.	CF massive MIMO systems provide a better converges than conventional collocated massive MIMO systems and uncoordinated small cells.	To expand the coverage for a greater number of user equipment (UEs), it is recommended to consider non-orthogonal downlink pilots. Additionally, there is a need for more advanced power control algorithms to improve the overall performance of the system.
(Ngo et al., 2017)	On the Total Energy Efficiency of	Numerous distributed APs with multiple antennas	Optimal power allocation algorithm to achieve the	The energy efficiency can be greatly enhanced by employing a	To minimize power consumption resulting from the backhaul links, AP selection schemes are employed

	Cell-Free Massive MIMO	simultaously serve numerous single-antenna users within the same time-frequency resource. To achieve this, a straightforward conjugate beamforming scheme is implemented at each AP, utilizing local CSI.	highest possible total energy efficiency while adhering to constraints on per-user spectral efficiency and per-AP power.	power allocation algorithm and selecting appropriate access points (APs). In the case of a specific user, only a limited number of APs are actively involved in providing service to that user.	where each user selects a subset of access points (APs).
(X. Zhang, X. Qiao, et al., 2022)	Reconfigurable Intelligent Surface-Aided Cell-Free Massive MIMO	By employing low-resolution ADCs, the secure aspect is enhanced in a cell-free	The APs and the RIS utilize the imperfect channel state information (CSI) that is accessible to implement	In order to address the issue of excessive overhead involved in uplink training, a straightforward and efficient	The presence of a non-zero channel estimation error floor is solely determined by the quantization distortion factor (quantization bits) of the low-resolution ADCs at the APs. This error floor cannot be

	with Low-Resolution ADCs: Secrecy Performance Analysis and Optimization	massive MIMO system assisted by RIS.	conjugate beamforming and random beamforming techniques for downlink data transmission, respectively to enhance the performance of the system.	method for aggregated channel estimation is introduced, allowing the acquisition of channel state information (CSI) at the APs. By utilizing the estimated CSI, conjugate beamforming is implemented at the APs.	reduced by increasing the number of APs or improving the signal-to-noise ratio (SNR).

This literature review highlights the significance of performance enhancement techniques for scalable cell-free massive MIMO systems, with a specific focus on the dynamic cooperation cluster optimization concept. It demonstrates the evolving research landscape in this field, ranging from architectural aspects to interference management and resource allocation strategies. The review reveals research gaps and challenges that need to be addressed, such as developing efficient algorithms for dynamic cluster formation, inter-cluster coordination, and resource allocation. The findings of this literature review provide valuable insights and serve as a foundation for the proposed research on enhancing the performance of scalable cell-free massive MIMO systems using dynamic cooperation cluster optimization

CHAPTER THREE

3. METHODOLOGY

3.1. Material

The study aims to investigate the performance enhancement of scalable cell free massive MIMO systems through the application of the dynamic cooperation cluster optimization concept. To achieve this, MATLAB 2021 will be employed for simulation and analysis purpose and it offers a comprehensive set of tools and function that are well-suited for this research.

3.2. Methods of the Study

The study will adopt a systematic approach to investigate the performance enhancement of scalable cell-free massive MIMO systems using the dynamic cooperation cluster optimization concept. The research design will involve a combination of theoretical analysis, simulation studies, and practical experiments to evaluate the effectiveness of the proposed approach. This will enable a comprehensive understanding of the benefits, limitations, and a practical consideration associated with implementing dynamic cooperation cluster optimization in cell-free massive MIMO systems is shown in Fig 3.1.

3.2.1. Simulation Methods

A simulation framework will be built in order to assess how well the suggested dynamic cooperative cluster optimization concept performs. Realistic network models that replicate the traits of scalable cell-free massive MIMO systems will make up the framework. Models for resource allocation, channel propagation, user mobility, and interference will all be included. Through the use of the simulation framework, the suggested strategy will be evaluated in a variety of settings and circumstances, enabling a thorough performance study. The effectiveness of the dynamic cooperative cluster optimization idea will be assessed through the analysis of data gathered from simulations and tests. Techniques for statistical analysis will be used to find trends and make intelligible conclusions. The suggested approach's efficacy in improving the performance of scalable cell-free massive MIMO systems will be evaluated by comparing the obtained results with baseline scenarios and current methodologies. The suggested approach's drawbacks and trade-offs will be noted and spoken about. This study will employ a comprehensive methodology that combines theoretical analysis, simulation studies, and experimental validation to investigate the performance enhancement of scalable cell-free massive MIMO systems using the dynamic cooperation cluster optimization concept

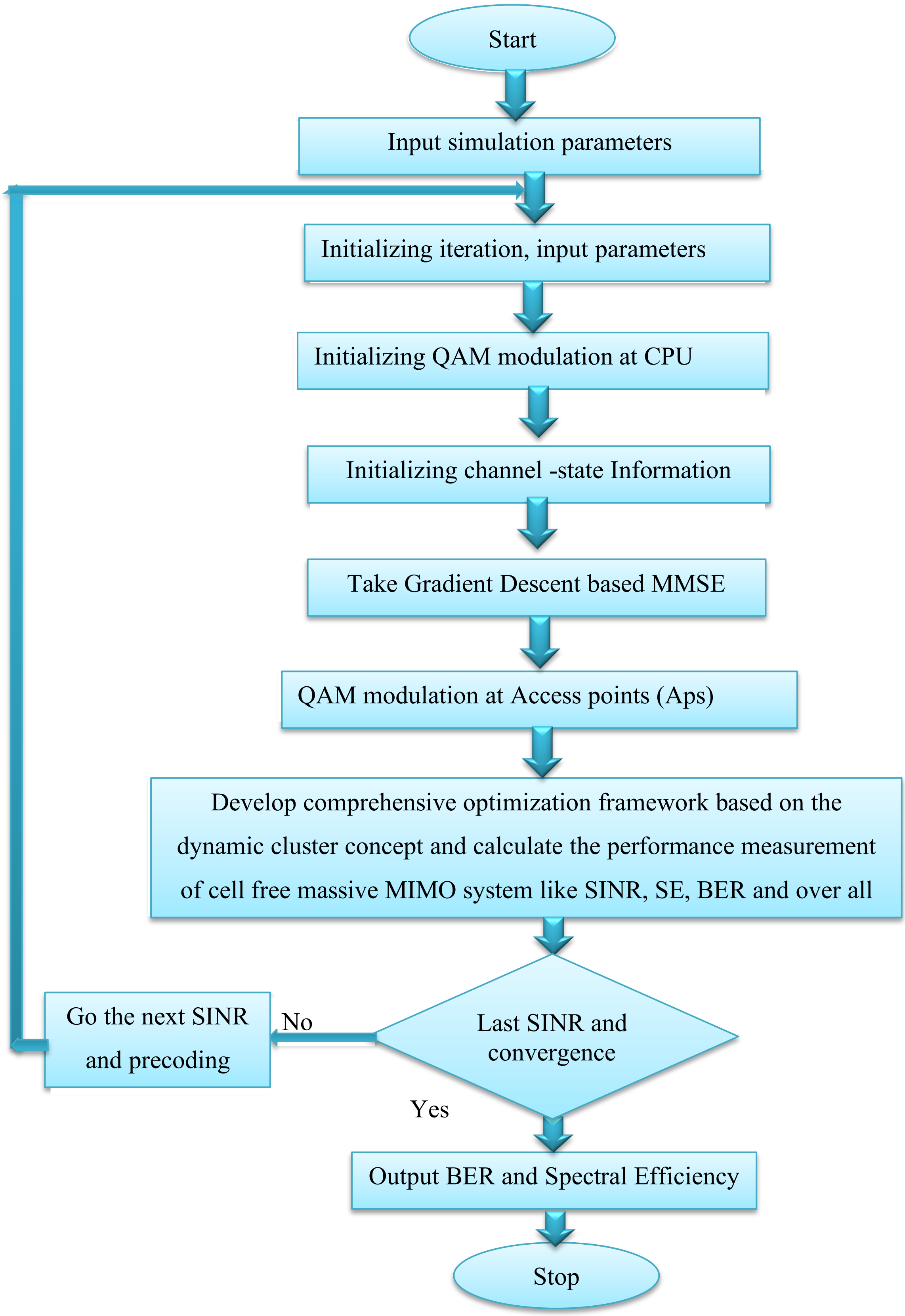

Figure 3. 1. Flow chart of proposed system

3.3. Block Diagram of a Scalable Massive MIMO System Architecture

The system being described is a cell-free massive MIMO setup with L access points (APs), each equipped with N antennas. The total number of AP antennas in the network is M = NL. There is K single-antenna user equipment (UEs) that are collectively served by the APs. Each UE communicates with a subset of the APs, selected based on the UE's requirements. The fronthaul links connecting the APs to the central processing units (CPUs) enable cooperation between the APs.

The signal transmitted from AP l in the downlink is represented by the vector $\mathbf{x}_l \in \mathbb{C}^N$, which has N complex-valued elements. The receiver noise for each user k is denoted by $n_k \sim \mathcal{N}_{\mathbb{C}}\left(0, \sigma_{\mathrm{dl}}^2\right)$, which follows a complex normal distribution with a mean of 0 and a variance of σ_{dl}^2. To represent the downlink channel, we use the Hermitian transpose of the channel vector $\mathbf{h}_{kl}^{\mathrm{H}}$, which has a superscript H. Although in practice, only the transpose of the channel vector is needed, the complex conjugate is included in the notation for simplicity, without affecting the system's performance.

Subsequently, based on (Björnson & Sanguinetti, 2020) the signal received by user k can be formulated as

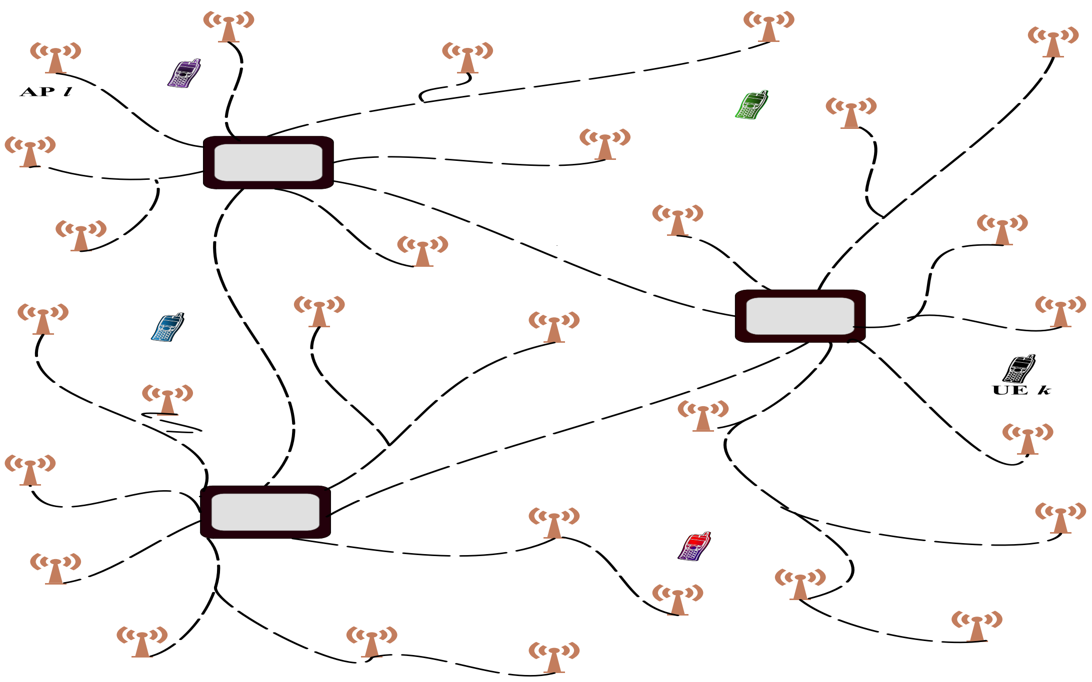

Figure 3. 2. Block Diagram of Scalable cell free Massive Network(Björnson & Sanguinetti, 2020)

$$y_k^{dl} = \sum_{l=1}^{L} h_{kl}^H x_l + n_k \tag{3.1}$$

$\varsigma_i \in \mathbb{C}^N$ is defined as the separate unit-power information signal intended for user i, hence $\mathbb{E}\{|\varsigma_i|^2\} = 1$. The transmitted signal by AP l is a constructed combination of the precoded signals that are designated for each of the supported UEs. In other words, this can be expressed as (Bjornson & Sanguinetti, 2019), (Björnson & Sanguinetti, 2020)

$$\mathbf{x}_l = \sum_{i=1}^{K} \mathbf{c}_{il}\mathbf{P}_{il}\varsigma_i \quad (3.2)$$

Where transmitted precoding vector assigned to UE *i* by AP *l* is indicated by the symbol$\mathbf{P}_{il} \in \mathbb{C}^N$. This vector's effects on the transmission are significant in two ways: The spatial directionality is determined by the direction $\mathbf{P}_{il}/\|\mathbf{P}_{il}\|$, and the averages transmit power is determined by the average squared norm $\mathbb{E}\{\|\mathbf{P}_{il}\|^2\}$. The efficient precoding vector can be described as

$$\mathbf{c}_{il}\mathbf{P}_{il} = \begin{cases} \mathbf{P}_{il} & l \in \mathcal{M}_i \\ \mathbf{0}_N & l \notin \mathcal{M}_i \end{cases} \quad (3.3)$$

Given that $\mathbf{c}_{il} = \mathbf{0}_{N\times N}$, $\mathbf{c}_{il}\mathbf{P}_{il} = \mathbf{0}_N$ is implied and $\mathcal{M}_i$ refers to APs found in the cluster. It follows that each AP simply has to choose the precoding vectors for the UEs under its support. Replacing the transmitted signal in equation (3.2) into equation (3.1) results in the downlink signal received at user k.

$$\begin{aligned} y_k^{\mathrm{dl}} &= \sum_{l=1}^{L} \mathbf{h}_{kl}^{\mathrm{H}} \left(\sum_{i=1}^{K} \mathbf{c}_{il}\mathbf{P}_{il}\varsigma_i\right) + n_k \\ &= \sum_{l=1}^{L} \mathbf{h}_{kl}^{\mathrm{H}}\mathbf{c}_{kl}\mathbf{P}_{kl}\varsigma_k + \sum_{\substack{i=1 \\ i\neq k}}^{K} \sum_{l=1}^{L} \mathbf{h}_{kl}^{\mathrm{H}}\mathbf{c}_{il}\mathbf{P}_{il}\varsigma_i + n_k \end{aligned} \quad (3.4)$$

In equation 3.1 the desired signal is the first term, followed by interference from users and noise.

3.4. SE of Centralized cell-free Downlink Data Transmission

By presenting this feasible expression, the goal is to provide a standardized and widely applicable approach to calculating spectral efficiency, simplifying the analysis and evaluation of various communication systems that employ different precoding techniques.

In order to assess the scalability of a cell-free network, it is crucial to observe the practical feasibility of certain tasks at each access point (AP) as the number of APs (K) approaches infinity. The following tasks need to be examined

1. Estimating the channel through signal processing.
2. Receiving and transmitting data through signal processing.
3. Sharing data and channel state information (CSI) through fronthaul signaling.
4. Optimizing power allocation.

By evaluating the practical implement ability of these tasks as K increases, one can determine whether a cell-free network can effectively scale and handle a large number of APs. The signal received by user equipment (UE) k in equation (3.4) can be split into three components and expressed in a revised form.

$$y_k^{\text{dl}} = \underbrace{\mathbf{h}_k^{\text{H}}\mathbf{c}_k\mathbf{P}_k s_k}_{\text{Desired signal}} + \underbrace{\sum_{\substack{i=1 \\ i\neq k}}^{K} \mathbf{h}_k^{\text{H}}\mathbf{c}_i\mathbf{P}_i s_i}_{\text{Inter-user interference}} + \underbrace{n_k}_{\text{Noise}}$$

(3.5)

The objective of the User Equipment (UE) is to obtain information from the initial component despite the presence of interference caused by other users and noise, as indicated in the subsequent two sections. The outcome of the desired signal *ςk* multiplied by the expression **h***k*H**c***k***P***k* is referred to as the effective downlink channel, which indicates that the precoding technique effectively converts the multi-antenna channel **h***k* into a single-antenna channel represented by **h***k*H**c***k***P***k*. According to (Ye et al., 2022)the achievable downlink DL spectral efficiency with user K is:-

$$\text{SE}_k^{(\text{dl,c})} = \frac{\tau_d}{\tau_c}\log_2\left(1+\text{SINR}_k^{(\text{dl,c})}\right)\text{bit / s / Hz} \tag{3.6}$$

Where $\text{SINR}_k^{(\text{dl,c})}$ is an effective SNIR of cell free massive MIMO network in downlink operation:-

$$SINR_k^{(\text{dl},c)} = \frac{\left|\text{E}\left\{\mathbf{h}_k^{\text{H}}\mathbf{c}_k\mathbf{P}_k\right\}\right|^2}{\sum_{i=1}^{K}\text{E}\left\{\left|\mathbf{h}_k^{\text{H}}\mathbf{c}_i\mathbf{P}_i\right|^2\right\} - \left|\text{E}\left\{\mathbf{h}_k^{\text{H}}\mathbf{c}_k\mathbf{P}_k\right\}\right|^2 + \sigma_{\text{dl}}^2} \tag{3.7}$$

The fraction of each coherence block allocated for downlink data transmission is represented by the pre-log factor τd/τc in equation (3.6)

❖ **Centralized Transmit Precoding**

The complexity of selecting transmit precoding vectors in Equation 3.7 is increased due to its dependence on the precoding of all User Equipment (UEs) within the network. This is denoted as follow.

$$\mathbf{P}_k = \sqrt{\rho_k}\frac{\overline{\mathbf{P}}_k}{\sqrt{\text{E}\left\{\left\|\overline{\mathbf{P}}_k\right\|^2\right\}}}$$

(3.8)

The parameter $\mathbf{P}_k$ (where $\mathbf{P}_k \geq 0$) represents the total transmit power allocated to User Equipment (UE) k by all the serving Access Points (APs). On the other hand, $\overline{\mathbf{P}}_k \in \mathbb{C}^{LN}$ is a scaled vector that indicates the direction of the precoding vector. It is important to observe that the normalization mentioned in equation (3.8) ensures that

$$\mathrm{E}\left\{\left\|\mathbf{P}_k\right\|^2\right\} = \rho_k$$

(3.9)

3.4.1. MMSE precoding

MMSE precoding is a more advanced technique that takes into accounts both interference and noise. The MMSE precoding vector in the downlink data transmission obtained from equation (3.8) (Papazafeiropoulos et al., 2021) defined as follow.

$$\overline{\mathbf{P}}_k^{\mathrm{MMSE}} = p_k \left(\sum_{i=1}^{K} p_i \mathbf{c}_k \left(\hat{\mathbf{h}}_i \hat{\mathbf{h}}_i^{\mathrm{H}} + \mathbf{R}_i \right) \mathbf{c}_k + \sigma_{\mathrm{dl}}^2 \mathbf{I}_{LN} \right)^{-1} \mathbf{c}_k \hat{\mathbf{h}}_k$$

(3.10)

MMSE precoding involves minimizing the total Mean Squared Error (MSE) between the vector of data signals and the received signal vector from all User Equipment (UEs).

The MMSE combining vector maximizes the Effective Signal-to-Interference-plus-Noise Ratio (SINR) for User Equipment (UE) k, as expressed in equation (3.7)(Tuğfe Demir et al., 2021).

$$SINR_k^{(\mathrm{dl},c)MMSE} = \mathbf{h}_k^{\mathrm{H}} \mathbf{c}_k p_k \left(\sum_{i=1}^{K} p_i \mathbf{c}_k \left(\hat{\mathbf{h}}_i \hat{\mathbf{h}}_i^{\mathrm{H}} + \mathbf{R}_i \right) \mathbf{c}_k + \sigma_{\mathrm{dl}}^2 \mathbf{I}_{LN} \right)^{-1} \mathbf{c}_k \hat{\mathbf{h}}_k$$

(3.11)

3.4.2. PMMSE precoding

In a distributed network with numerous UEs and extensive coverage, it is reasonable to assume that the interference impacting UE k primarily originates from a limited number of neighboring UEs. We aim to leverage this observation in order to decrease the computational complexity associated with the optimal Minimum Mean Square Error (MMSE) percoding process. By doing so, we can achieve a scalable alternative approach.

The alternative Scalable MMSE precoding vector which is PMMSE vector is given as follow(Mai et al., 2020)

$$\overline{\mathbf{P}}_k^{\mathrm{PMMSE}} = p_k \left(\sum_{i \in \mathrm{S}_k} p_i \mathbf{c}_k \hat{\mathbf{h}}_i \hat{\mathbf{h}}_i^{\mathrm{H}} \mathbf{c}_k + \mathbf{R}_{\delta_k} + \sigma_{\mathrm{dl}}^2 \mathbf{I}_{LN} \right)^{-1} \mathbf{c}_k \hat{\mathbf{h}}_k$$

(3.12)

The PMMSE combining vector maximizes the Effective Signal-to-Interference-plus-Noise Ratio (SINR) for User Equipment (UE) k, as expressed in equation (3.7).

$$SINR_k^{(\mathrm{dl},c)PMMSE} = \mathbf{h}_k^{\mathrm{H}}\mathbf{c}_k p_k \left(\sum_{i \in \mathrm{S}_k} p_i \mathbf{c}_k \hat{\mathbf{h}}_i \hat{\mathbf{h}}_i^{\mathrm{H}} \mathbf{c}_k + \mathbf{R}_{\delta_k} + \sigma_{\mathrm{dl}}^2 \mathbf{I}_{LN} \right)^{-1} \mathbf{c}_k \hat{\mathbf{h}}_k$$

(3.13)

3.4.3. PRZF precoding

Zero Forcing precoding: aims to eliminate interference among different communication streams. To reduce the computational complexity of MMSE technique has an alternative method is derived from simplifying PMMSE technique. This approach entails disregarding the estimation error correlation matrix $\mathbf{R}\mathcal{S}k$ in equation (3.12). Partial Regularized Zero Forcing (PRZF) precoding can be obtained by applying equation (3.11) in the subsequent manner (Ye et al., 2022).

$$\bar{\mathbf{P}}_k^{\mathrm{PRZF}} = \left[\mathbf{c}_k \hat{\mathbf{h}}_{\delta_k} \left(\hat{\mathbf{h}}_{s_k}^{\mathrm{H}} \mathbf{c}_k \hat{\mathbf{h}}_{s_k} + \sigma_{\mathrm{dl}}^2 p_{s_k}^{-1} \right)^{-1} \right]_{;,1}$$

(3.15)

In this context, it is important to note that the matrix $\hat{\mathbf{h}}_{s_k} \in \mathbb{C}^{LN \times |S_k|}$ is obtained by arranging all the vectors $\hat{\mathbf{h}}_i$ with indices $i \in S_K$, where the first column represents $\hat{\mathbf{h}}_k$. Additionally, $P_{SK} \in \sim^{|S_K| \times |S_K|}$ is a diagonal matrix that contains the transmit powers pi for i ∈ Sk, arranged in the same order as the columns of $\hat{\mathbf{h}}_k$. Then we can employ P-RZF precoding in the downlink without any additional computational complexity. This characteristic contributes to the scalability of the precoding scheme. The Effective Signal-to-Interference-plus-Noise Ratio (SINR) of PRZF precoding for User Equipment (UE) k, as expressed in equation (3.7) is.

$$SINR_k^{(\mathrm{dl},c)PRZF} = \mathbf{h}_k^{\mathrm{H}}\mathbf{c}_k p_k \left[\mathbf{c}_k \hat{\mathbf{h}}_{\delta_k} \left(\hat{\mathbf{h}}_{s_k}^{\mathrm{H}} \mathbf{c}_k \hat{\mathbf{h}}_{s_k} + \sigma_{\mathrm{dl}}^2 p_{s_k}^{-1} \right)^{-1} \right]_{;,1}$$

(3.16)

3.5. Downlink Operation in a Distributed System

The tasks related to downlink signal processing can be allocated differently between the access points (APs) and the central processing unit (CPU). In a distributed operation, all tasks except data encoding are performed at the APs. The central processing unit (CPU) performs data encoding for the downlink data signals $\{\varsigma_i$: i = 1, 2 . . ., K$\}$ and transmits them to the respective serving access points (APs). The access points (APs) are responsible for conducting the remaining signal processing tasks.

The distributed operation offers a significant advantage in that the deployment of new access points (APs) does not necessitate an upgrade in the computational capabilities of the central processing unit (CPU). This is because each AP is equipped with its own local processor capable of performing the necessary baseband processing tasks. In the distributed operation, (Chen et al., 2020) each AP independently designs its transmitted signal locally.

$$X_l = \sum_{i=1}^{k} c_{il} p_{il} \varsigma_i$$

(3.17)

3.6. Spectral Efficiency in a Distributed Downlink Operation

UE k receives the signal from the access point (AP) can be expressed as follow.

$$\begin{aligned} y_k^{\mathrm{dl}} &= \sum_{l=1}^{L} \mathbf{h}_{kl}^{\mathrm{H}} x_l + n_k \\ &= \sum_{l=1}^{L} \mathbf{h}_{kl}^{\mathrm{H}} \left(\sum_{i=1}^{K} \mathbf{c}_{il} \mathbf{P}_{il} \varsigma_i \right) + n_k \\ &= \sum_{l=1}^{L} \mathbf{h}_{kl}^{\mathrm{H}} \mathbf{c}_{kl} \mathbf{P}_{kl} \varsigma_k + \sum_{\substack{i=1 \\ i \neq k}}^{K} \sum_{l=1}^{L} \mathbf{h}_{kl}^{\mathrm{H}} \mathbf{c}_{il} \mathbf{P}_{il} \varsigma_i + n_k \end{aligned}$$

(3.18)

This scenario is similar to the centralized downlink operation described in (3.4). However, the main distinction lies in the selection of precoding, which is now performed locally at each access point (AP) using the channel estimates available at that particular AP.

The achievable spectral efficiency (SE) for UE k in the distributed downlink operation is

$$\mathrm{SE}_k^{(\mathrm{dl},d)} = \frac{\tau_d}{\tau_c} \log_2 \left(1 + \mathrm{SINR}_k^{(\mathrm{dl,c})} \right) \mathrm{bit/s/Hz}$$

(3.19)

Where the Effective SNIR value from equation 3.7 also given by

$$SNIR_k^{(dl,d)} = \frac{\left| \sum_{l=1}^{L} \mathrm{E}\left\{ \mathbf{h}_{kl}^{\mathrm{H}} \mathbf{c}_{kl} \mathbf{P}_{kl} \right\} \right|^2}{\sum_{i=1}^{K} \mathrm{E}\left\{ \left| \mathbf{h}_{kl}^{\mathrm{H}} \mathbf{c}_{il} \mathbf{P}_{il} \right|^2 \right\} - \left| \mathrm{E}\left\{ \mathbf{h}_{kl}^{\mathrm{H}} \mathbf{c}_{kl} \mathbf{P}_{kl} \right\} \right|^2 + \sigma_{\mathrm{dl}}^2}$$

(3.20)

❖ Local Precoding Vector

In the distributed downlink operation, only a portion of the access points (APs) transmit a downlink data signal to a specific UE k. Therefore, it is sufficient to select the effective precoding vectors $\mathbf{c}_{kl}\mathbf{P}_{kl}$ for the APs in the subset M_k.When an AP L serves UE (k), the precoding vector can be expressed as follows:

$$\mathbf{P}_{kl} = \sqrt{\rho_{kl}} \frac{\overline{\mathbf{P}}_{kl}}{\sqrt{\mathrm{E}\left\{\left\|\overline{\mathbf{P}}_{kl}\right\|^2\right\}}} \tag{3.21}$$

The transmit power assigned by AP l to UE k is denoted as $p_{kl} \geq 0$, and the direction of the precoding vector is represented by $\overline{\mathbf{P}}_{kl}$, which is an arbitrarily scaled vector in the complex number space.

3.6.1. LMMSE precoding

The L-MMSE precoding, which serves as the counterpart for the downlink, is derived from equation (3.21).

$$\overline{\mathbf{P}}_k^{\mathrm{PMMSE}} = p_k \left(\sum_{i=1}^{k} p_i \left(\hat{\mathbf{h}}_{il}\hat{\mathbf{h}}_{il}^{\mathrm{H}} + \mathbf{R}_{il} \right) + \sigma_{\mathrm{dl}}^2 \mathbf{I}_{LN} \right)^{-1} \mathbf{c}_{kl}\hat{\mathbf{h}}_{kl} \tag{3.22}$$

Due to its strong association with the L-MMSE combining method, we anticipate that this precoding technique will yield the highest spectral efficiency among the various distributed alternatives (Zhang et al., 2019).

3.6.2. LPMMSE precoding

By focusing solely on the user equipment (UE) that is served by the access point (AP), we can attain a scalable approximation of L-MMSE precoding, we call this LP-MMSE precoding and obtain it from (3.21). The LPMMSE precoding vector is defined as follow.

$$\overline{\mathbf{P}}_k^{\mathrm{PMMSE}} = p_k \left(\sum_{i \in c_l} p_{il} \left(\hat{\mathbf{h}}_{il}\hat{\mathbf{h}}_{il}^{\mathrm{H}} + \mathbf{R}_{il} \right) + \sigma_{\mathrm{dl}}^2 \mathbf{I}_{LN} \right)^{-1} \mathbf{c}_{kl}\hat{\mathbf{h}}_{kl} \tag{3.23}$$

3.7. Dynamic Clustering of Cooperation (DCC)

Dynamic cooperation clusters in cell-free downlink operation offer numerous advantages (Björnson & Sanguinetti, 2019b; Sheikh et al., 2023; Zhang et al., 2019).

1. Improve interference management by facilitating coordinated transmissions among Aps.
2. Reducing interference and enhancing spectral efficiency.
3. The clusters' dynamic nature enables adaptive resource allocation, allowing APs to flexibly modify their cooperation strategies in response to evolving network conditions and UE needs.

The establishment and coordination of dynamic cooperation clusters in cell-free downlink operation can be guided by diverse algorithms and optimization techniques. These methods consider factors such as channel state information, user demand, power limitations, and fairness concerns to optimize both cluster formation and resource allocation among APs.

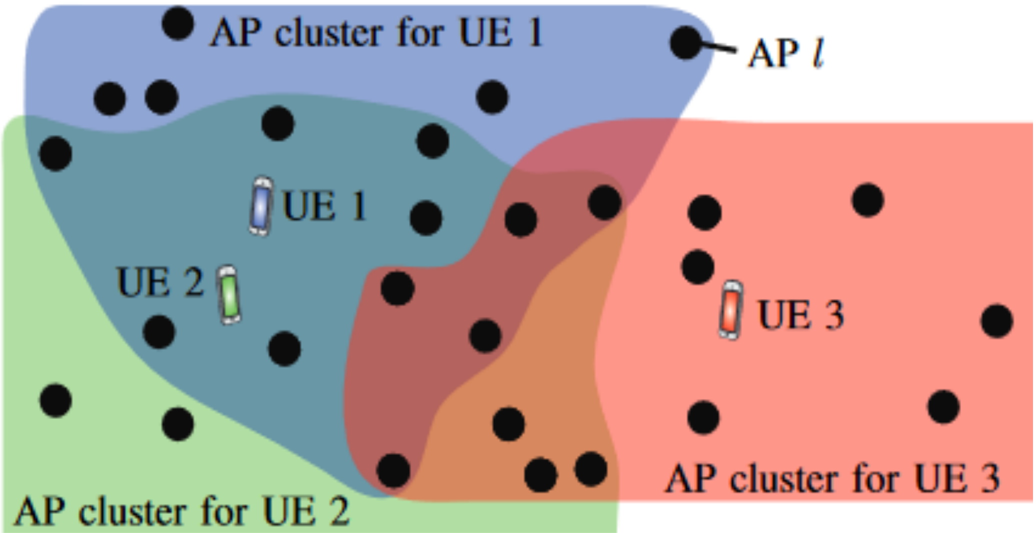

Figure 3. 3: Indicates a dynamic clustering cooperation involving a large number of access points and three UEs (Demir et al., 2021; Interdonato et al., 2019).

3.8. Proposed Method

The main objective of this thesis is to develop a proficient precoding method by utilizing the current precoding algorithm as a foundation.

To ensure high data rates and minimize interference in cell-free massive MIMO networks, efficient precoding techniques play a crucial role. Precoding involves manipulating the transmitted signals at access points (APs) to align them with the intended user equipment (UEs) while minimizing interference to other UEs. One commonly used technique is Minimum Mean Square Error (MMSE) precoding, which aims to minimize the mean square error between the desired and received signals at each UE.

Traditionally, solving the optimization problem associated with MMSE precoding in cell-free massive MIMO relied on conventional techniques like linear programming or convex optimization. However, these methods can be computationally intensive, especially when dealing with a large number of APs and UEs. Therefore, there is a need to explore more computationally efficient optimization algorithms for MMSE precoding in cell-free massive MIMO systems.

- **Gradient descent** is a popular optimization algorithm widely employed in machine learning and signal processing. It is an iterative method that seeks to find the minimum of a cost function by progressively updating parameters in the direction of the steepest descent. In recent years, the application of gradient descent in wireless communication systems has demonstrated promising results, such as enhanced convergence speed and reduced computational complexity (Dong et al., 2018).

The gradient descent algorithm can be utilized to optimize PMMSE precoding in cell-free massive MIMO systems by continuously adjusting the precoder parameters in the direction that minimizes the cost function. Let's delve into how the algorithm operates specifically for MMSE precoding optimization.

- Start by initializing the precoding matrix $\overline{p}$ with initial values.
- Specify the maximum number of iterations as i_{Max}
- Assume and Set the convergence threshold as ε =0.0001
- Set the iteration counter Iteration $i = 0$.
- Calculate the initial MSE as MSE_{old} using the compute of $MSE(\overline{p})$ function.
- Repeat the following steps until convergence or reaching the maximum number of iterations:
  - ✓ Increase the iteration counter: $i = i + 1$
  - ✓ Compute the gradient of MSE with respect to $\overline{p}$ as gradient using compute $Gradient(\overline{p})$ function.
  - ✓ Update the precoding matrix: $\overline{p} = \overline{p} - \eta * gradient(\overline{p})$ where η represents the learning rate. Assuming small learning rate values which is between 0.01 and 0.05. we consider 0.0125 value of learning rate.
  - ✓ Calculate the new MSE as MSE_{New} using the compute $MSE(\overline{p})$ function.
  - ✓ Check for convergence: if the absolute difference between MSE_{New} and MSE_{old} is smaller than ε, exit the loop.
  - ✓ Update MSE_{old} with the value of MSE_{New}.
  - ✓ If the iteration counter Iteration i is greater than or equal to i_{Max}, exit the loop.
- Retrieve the optimized precoding matrix $\overline{p}$ as the output.

As defined in equation 3.1 the signal received by user k formulated as follow: -

$$y_k^{dl} = \sum_{l=1}^{L} h_{kl}^H x_l + n_k \tag{3.24}$$

Where $x_l = \sum_{i=1}^{k} c_{il} p_{il} \varsigma_{il}$

In downlink massive MIMO system MMSE precoding vector (Dong et al., 2018)is expressed as follow:-

$$p = H^H (\mathrm{HH}^H + \delta^2 I_K)^{-1} \quad (3.25)$$

Where $W = (\mathrm{HH}^H + \delta^2 I_K)$, subsequently, the signal vector x that has undergone pre-coding is determined as follow.

$$x = ps = H^H W^{-1} s = H^H \hat{s} \quad (3.26)$$

Where $\hat{s} = W^{-1} s$, s represents the vector of the transmitted signals from all k users.

The use of PMMSE precoding in massive MIMO systems presents significant challenges in practical applications due to the intricate matrix inversion operation involved, which has a complexity of M^3. Then find the mean squared error by calculating the squared difference between the desired signal x and the received signal y by utilizing current PMMSE precoding vector.

$$MSE = E\left[(x-y)^H (x-y)\right] \quad (3.27)$$

$$MSE = E\left[(x - HP_{MMSE})^H (x - HP_{MMSE})\right] \quad (3.28)$$

Then the gradient of MSE with respect to the precoding matrix of MMSE precoding after mathematical solution, the gradient of MSE is defined as follow: -

$$MSE(p)_{gradient} = -2E\left[H^H (x - H * P_{MMSE})\right] \quad (3.29)$$

Adjust the precoding matrix P by incorporating the gradient and a learning rate η.

$$p_{new} = p - \eta * MSE(p)_{gradient} \quad (3.30)$$

Where p_{new} updated precoding matrix of MMSE precoding in the downlink operation.

Algorithm 1: pseudo-code for proposed precoding scheme based on MMSE precoding with GD optimizer stated as follow:

Input:

Initialize $P_{MMSE}, H, x, \varepsilon, \eta, i_{Max}, i = 0$

While $i \le i_{Max}$

Calculate p_{MMSE} based on equation (3.25)

Compute MSE based on equation (3.28)

Calculate the gradient based on equation (3.29)

Update precoding matrix based on equation (3.30)

Increment the iteration

Output: $p_{Optimized} = p$

End

3.9. Block Diagram of Proposed Method

The block diagram of the proposed method can be described in the form of block diagram as Figure 3.3. Precoding techniques play a crucial role in modern communication systems, particularly in wireless communication, where the transmission environment can be highly variable and challenging. Precoding refers to the manipulation of the transmitted signal at the transmitter to enhance the overall communication performance. The primary goal of precoding is to mitigate the effects of interference, improve spectral efficiency, and enhance the reliability of communication systems.

Dynamic Cooperation Cluster Optimization is a cutting-edge approach in wireless communication networks that enhances resource allocation and network efficiency. By dynamically forming and optimizing clusters of cooperating nodes, this technique adapts to changing network conditions in real-time, improving overall system performance. It enables nodes to collaboratively share information, allocate resources efficiently, and minimize interference, leading to enhanced reliability and throughput.

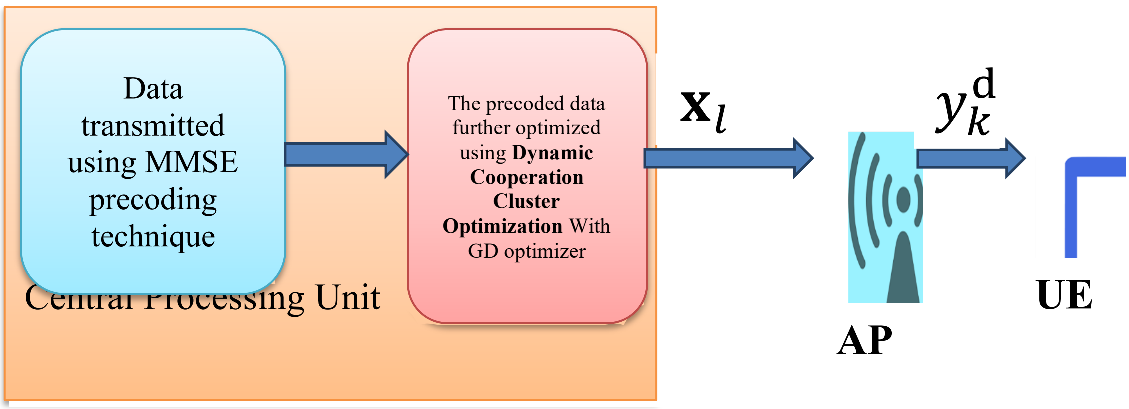

Figure 3. 4. Block diagram of proposed based on Dynamic Cooperation Cluster Optimization concept

The dynamic nature of cooperation clusters ensures adaptability to varying network scenarios, making it a valuable tool for optimizing communication in dynamic and complex wireless environments. This innovative optimization strategy contributes to the evolution of next-generation wireless networks.

CHAPTER FOUR

4. Results and Discussions

In order to demonstrate the effectiveness of user-centric cell-free massive MIMO in practical scenarios, we will introduce a network configuration that will be continuously referred to in this thesis. The key parameters are provided in Table 4.1. The coverage area encompasses either a 1 km × 1 km or a 2 km × 2 km region, while the number of antennas is determined by M = LN = 400, M=800, or M=1200. The number of access points (APs) can be either L = 400, L=200, or L = 100, and each AP is equipped with N = 1, N = 2, or N=3 antennas. To simulate a large-scale network deployment without any boundaries, we employ a wrap-around topology where all APs and users experience interference from every direction. The assumption is made that the access points (APs) are deployed randomly and uniformly across the coverage area of the network. The communication takes place within a 20 MHz bandwidth, and the combined noise power for both APs and user equipment (UEs) is -94 dBm. This noise power includes thermal noise and accounts for a 7 dB noise figure in the receiver hardware. Each AP is allowed to transmit a maximum power of 100 mW in the downlink. A coherence block of τc = 200 samples is utilized, which corresponds to a coherence bandwidth of 100 KHz and a coherence time of two milliseconds.

Table 4. 1: Simulation Parameters (Björnson & Sanguinetti, 2019b; Sheikh et al., 2023; Zhang et al., 2019; Zheng et al., 2022)

No.	Parameters	Value or Type
1	Network area	1 km^2
2	Network layout	Random deployment
3	The number of APs used	400
4	The number of antennas assigned to each AP	1, 2, 3 and 4
5	Total number of antennas	400, 800, 1200 and 1600
6	Bandwidth	20 MHz
7	Noise power of receiver	σdl^2 = -94 dBm
8	Highest transmit power in the downlink	100 mW
9	The number of samples in each coherence block.	τ_c =200
10	Gain at 1 km distance	Y= -140.6 dB
11	Exponent in the pathloss model	α =3.67
12	Height separation between UE and AP	10 m
13	Standard deviation of shadow fading	σsf = 4
14	Channel	Rayleigh fading

4.1. Performance comparrision of Scalable precoding with the Existing precoding

In order to evaluate and compare the performance of the suggested precoder with other precoding techniques currently in use, various factors are considered. These factors include average spectral efficiency, sum spectral efficiency, and cumulative distribution function. These parameters offer valuable understanding of the efficiency and effectiveness of different precoding methods, enabling a thorough assessment and comparison of their performance.

4.1.1. Performance comparrision of Scalable precoding with the Scalable precoding based on Average Spectral efficiency

In this section, our main objective is to measure the average spectral efficiency in the downlink for scalable user-centric cell-free massive MIMO. We will evaluate different precoding techniques, including the proposed method, along with existing techniques mentioned in Chapter Three. By comparing these approaches, we aim to understand the performance variations and assess the effectiveness of the proposed scheme. The simulations conducted in this thesis focus on evaluating the performance of the proposed algorithm against recently developed cell-free massive MIMO precoders. The performance measurement utilized is spectral efficiency, considering different numbers of user equipment (UE) and antennas per access point (AP). For generating these simulation outcomes, we employ the MATLAB software, which offers a robust platform for conducting simulations, implementing algorithms, and analyzing system performance. MATLAB facilitates the execution of simulations and the derivation of average spectral efficiency values, enabling a thorough comparison between the proposed algorithm and other cell-free Massive MIMO precoders in downlink transmission.

Figure 4.1 compares the Average DL SE per user equipment (UE) for the proposed method with other centralized and distributed precoding techniques. The analysis is conducted at a specific scenario with L = 400 and N = 1, implemented in a 1 km2 area. The main aim of this figur is to evaluate and compare the performance of different precoding techniques in terms of spectral efficiency. Based on the analysis, the proposed method for precoding demonstrates higher spectral efficiency compared to the other techniques. This implies that the proposed method is more effective in maximizing the data transmission capabilities per user equipment in the given scenario.

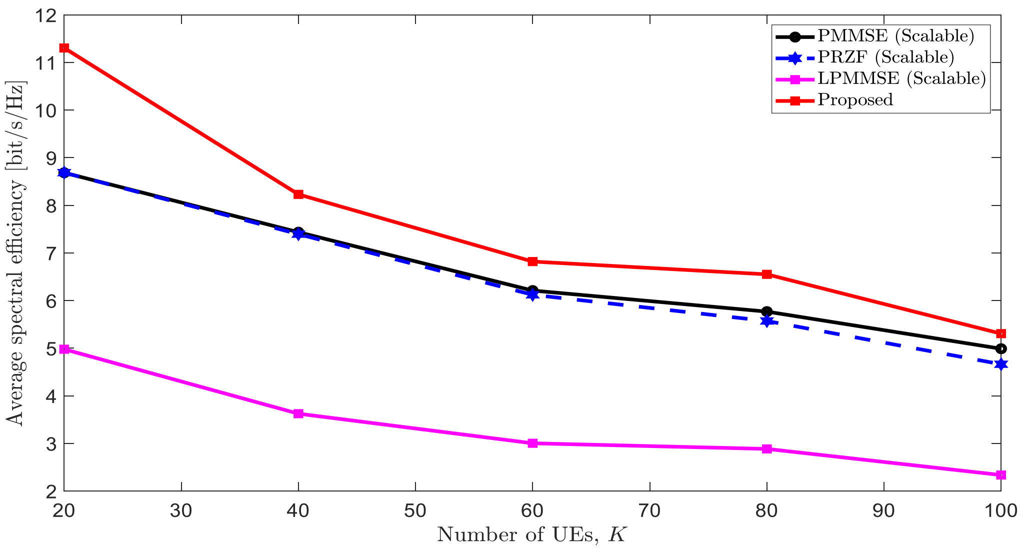

Figure 4. 1. Average DL SE per UE with different scalable and proposed precoding schemes at L=400 and N=1 in a 1km^2 region.

The three schemes are PMMSE (Scalable), PRZF (Scalable), and LPMMSE (Scalable). The proposed scheme outperforms the other schemes in terms of average spectral efficiency. The proposed precoding technique demonstrates superior performance compared to the other centralized and distributed precoding techniques in terms of Average DL SE. At UE=20, the average spectral efficiency for LPMMSE is 4.0842, for PRZF it is 8.405, for PMMSE it is 8.4205, and for the proposed technique it is 9. 274. At UE=100, the average spectral efficiency for LPMMSE is 2.3108, for PRZF it is 4.464, for PMMSE it is 4.776, and for the proposed technique it is 5.2456. This suggests that the proposed technique can effectively maximize data transmission capabilities per user equipment, even in scenarios with a high number of users.

Here is Table 4.2 demonstrating the Average DL SE per user equipment (UE) for the proposed method compared to other centralized and distributed precoding techniques at L = 400 and N = 1, implemented in a 1 km2 area:

Table 4. 2: Average DL SE per UE with different scalable and proposed precoding schemes at L=400 and N=1 in a 1km^2 region..

Average DL SE per user equipment (UE)					
S.No	No.UE	LPMMSE	PRZF	PMMSE	Proposed
1	20	4.0842	8.405	8.4205	9.274
2	40	3.715	7.3145	7.902	8.754
3	60	3.454	6.843	6.928	7.693
4	80	3.0173	6.406	6.624	7.524
5	100	2.3108	4.464	4.776	5.2456

This table provides the average spectral efficiency achieved by each precoding technique for different numbers of user equipments (UEs). The techniques include LPMMSE, PRZF, PMMSE, and the Proposed method. The values in the table represent the Average DL SE per UE. The proposed precoding technique consistently outperforms the other three techniques in terms of average spectral efficiency for all numbers of UEs.The average spectral efficiency generally decreases as the number of UEs increases for all precoding techniques. This is because the available bandwidth needs to be shared among more users, leading to reduced efficiency. The LPMMSE precoding technique performs the worst among the four techniques, especially at higher numbers of UEs. The PRZF and PMMSE precoding techniques have similar performance, with the PMMSE technique slightly outperforming the

PRZF technique at most numbers of UEs. The proposed precoding technique demonstrates superior performance compared to the other centralized and distributed precoding techniques in terms of Average DL SE. This suggests that the proposed technique can effectively maximize data transmission capabilities per user equipment, even in scenarios with a high number of users.

Figure 4.2 compares the Average DL SE per user equipment (UE) for the proposed precoding method and other scalable precoding techniques. The comparison is conducted at system parameters of L = 400 and N = 2, implemented in a 1 km2 area. At UE = 20, the Average DL SE per user equipment (UE) for the proposed method is 14.115, while for LPMMSE, PRZF, and PMMSE techniques, the values are 6.216, 9.189, and 9.233, respectively.

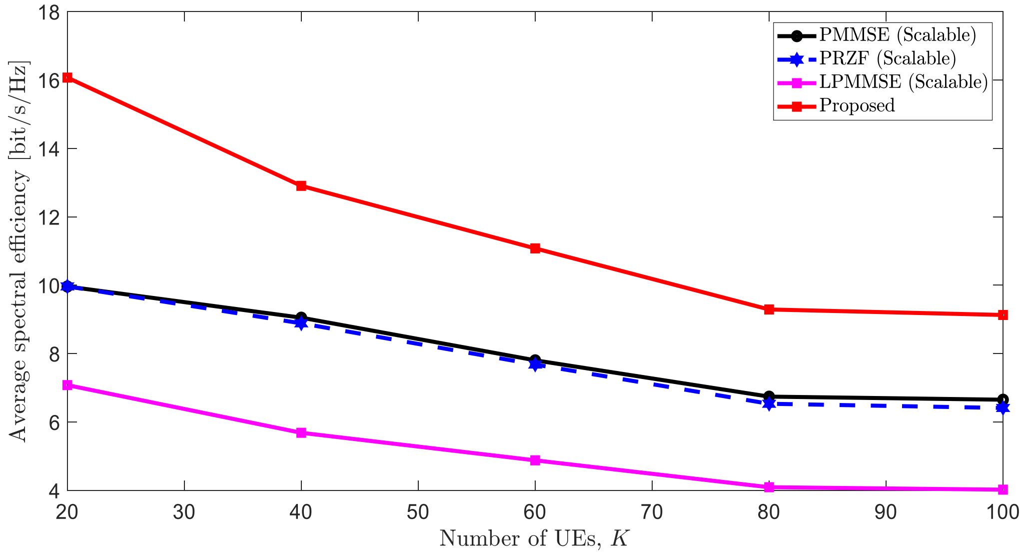

Figure 4. 2. Average DL SE per UE with different scalable and proposed precoding schemes at L=400 and N=2 in a 1km^2 region.

At UE = 100, the Average DL SE per user equipment (UE) for the proposed method is 9.106, while for LPMMSE, PRZF, and PMMSE techniques, the values are 4.012, 6.255, and 6.481, respectively. These results indicate that the proposed method outperforms the other scalable precoding schemes in terms of average DL SE for both UE levels.

Table 4. 3: Average DL SE per UE with different scalable and proposed precoding schemes at L=400 and N=2 in a 1km^2 region.

Average DL SE per user equipment (UE)					
S.No	No. UE	LPMMSE	PRZF	PMMSE	Proposed
1	20	6.216	9.189	9.233	14.115
2	40	5.456	8.902	9.028	13.682
3	60	4.753	8.654	8.804	11.743
4	80	4.387	7.621	8.261	10.642
5	100	4.012	6.255	6.481	9.106

Table 4.3 presents a comparison of the Average DL SE per user equipment (UE) for the proposed precoding method with other centralized and distributed precoding techniques. The comparison is conducted at system parameters of L = 400 and N = 2, implemented in a 1 km2 area. The proposed precoding method consistently outperforms the other techniques in terms of Average DL SE across all UE levels. At UE = 20, the proposed method achieves a significantly higher average spectral efficiency of 14.115 compared to LPMMSE = 6.216bit/s/Hz, PRZF = 9.189 bit/s/Hz, and PMMSE = 9.233 bit/s/Hz. As the UE level increases, the Average DL SE decreases for all techniques, but the proposed method consistently maintains the highest efficiency compared to the other techniques. LPMMSE exhibits the lowest average spectral efficiency among the compared methods for all UE levels. The PRZF and PMMSE techniques demonstrate relatively close performance, with the proposed method consistently surpassing both techniques.

Figure 4.3 illustrates the Average DL SE per user equipment (UE) for the proposed method compared to other scalable precoding techniques. The comparison is conducted at system parameters of L = 400, N = 3 and in a 1 km2 region. Based on the figure, it can be observed that the proposed method consistently outperforms the other techniques in terms of Average DL SE across all UE levels. At each UE level, the proposed method achieves higher spectral efficiency compared to LPMMSE, PRZF, and PMMSE.

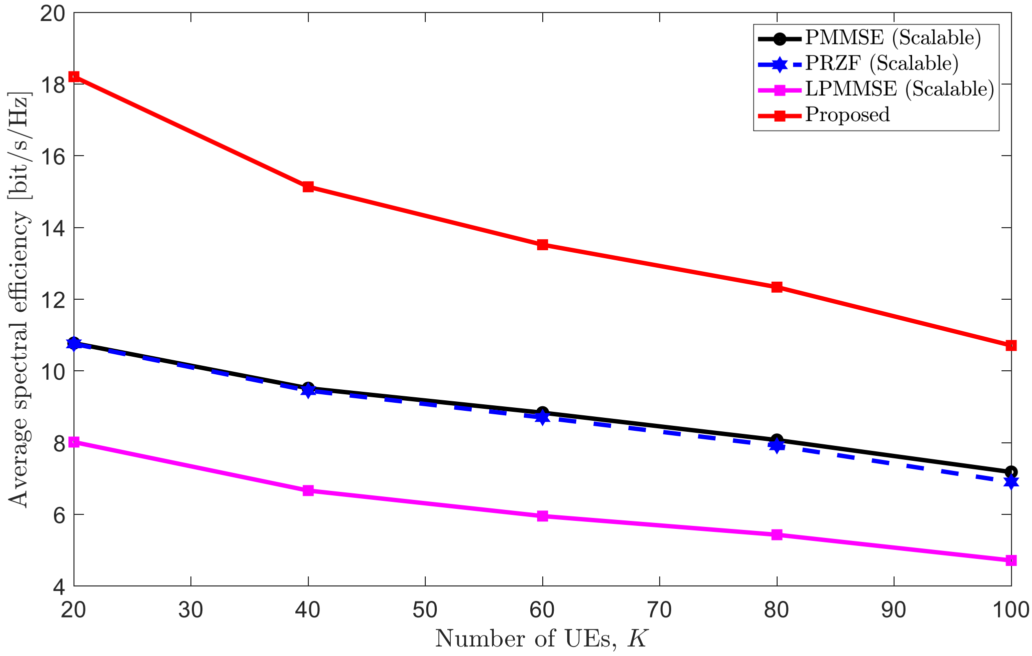

Figure 4. 3. Average DL SE per UE with different scalable and proposed precoding schemes at L=400 and N=3 in a 1km^2 region.

Furthermore, the figure highlights specific observations, such as the significantly higher spectral efficiency achieved by the proposed method at UE = 20 compared to the other techniques. It also indicates that as the UE level increases, the spectral efficiency decreases for all techniques, but the proposed method consistently maintains the highest efficiency compared to the others. The proposed method holds promise for improving the spectral efficiency in cell-free massive MIMO networks, providing a valuable contribution to the field of wireless communication and network optimization.

Table 4. 4: Average DL SE per UE with different scalable and proposed precoding schemes at L=400 and N=3 in a 1km^2 region.

Average DL SE per user equipment (UE)					
S.No	No. UE	LPMMSE	PRZF	PMMSE	Proposed
1	20	8.0173	10.7547	10.7754	18.2049
2	40	7.0126	9.8762	9.9012	15.0123
3	60	6.2174	9.4216	9.5012	14.1214
4	80	5.8208	8.8901	9.0341	13.6827
5	100	4.7168	6.9044	6.4808	10.7103

Table 4.4 presents the Average DL SE per user equipment (UE) for the proposed method compared to other scalable precoding techniques. The comparison is made at system parameters of L = 400, N = 3 in a 1 km^2 region. At UE level 20, the proposed method achieves an average spectral efficiency of 18.2049, while LPMMSE, PRZF, and PMMSE achieve 8.0173, 10.7547, and 10.7754, respectively. As the UE level increases to 40, 60, 80, and 100, the spectral efficiency decreases for all techniques. However, the proposed method consistently maintains the highest spectral efficiency among the compared techniques. For instance, at UE level 100, the proposed method achieves an average spectral efficiency of 10.7103, while LPMMSE, PRZF, and PMMSE achieve 4.7168, 6.9044, and 6.4808, respectively. This table provides a quantitative comparison of the Average DL SE for the proposed method and other precoding techniques, showing the superiority of the proposed method in terms of spectral efficiency across different UE levels.

Figure 4.4 presents a comparison of the Average DL SE per user equipment (UE) for the proposed method and other scalable precoding techniques. The evaluation is conducted in a specific scenario with L = 400 and N = 4, within a 1 km2 region. Analyzing the figure, we can observe the differences in performance among the precoding techniques. The proposed method consistently achieves higher average DL SE values compared to the other techniques across all UE levels.

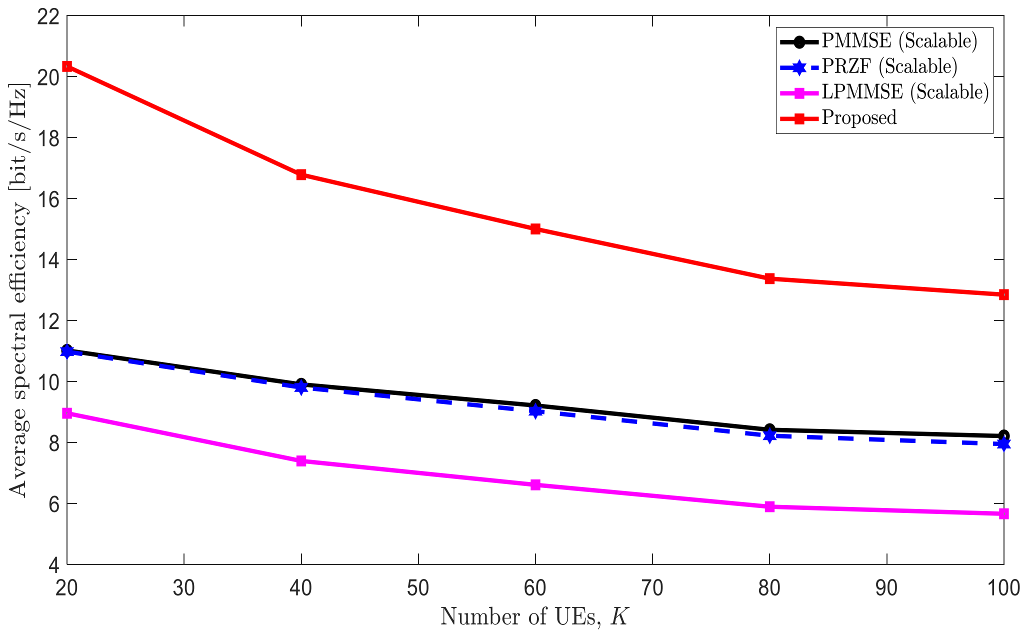

Figure 4. 4. Average DL SE per UE with different scalable and proposed precoding schemes at L=400 and N=4 in a 1km^2 region.

For instance, at UE 20, the spectral efficiency values are: LPMMSE = 8.9537bit/s/Hz, PRZF = 10.975bit/s/Hz, PMMSE = 11.0135bit/s/Hz and the Proposed method = 20.331bit/s/Hz. Similarly, at higher UE levels, such as UE 100, the proposed method achieves an average spectral efficiency value of 12.8438bit/s/Hz, outperforming LPMMSE, PRZF, and PMMSE techniques, which range from 5.6564bit/s/Hz to 8.2062bit/s/Hz. Based on these results, it can be concluded that the proposed method demonstrates superior performance in terms of Average DL SE per user equipment compared to other centralized and distributed precoding techniques at L = 400 and N = 4. These findings suggest that the proposed method has the potential to optimize downlink spectral efficiency in a 1 km2 area, considering the specified system parameters.

Table 4. 5: Average DL SE per UE with different scalable and proposed precoding schemes at L=400 and N=4 in a 1km^2 region.

Average DL SE per user equipment (UE)					
S.No	No.UE	LPMMSE	PRZF	PMMSE	Proposed
1	20	8.9537	10.975	11.0135	20.331
2	40	7.0126	10.2601	10.261	16.564
3	60	6.2174	9.6421	9.6421	15.652
4	80	5.8208	9.267	8.867	14.7253
5	100	5.6564	7.9436	8.2062	12.8438

Table 4.5 compares the Average DL SE per user equipment (UE) for different precoding techniques in a specific scenario. The scenario involves a 1 km2 area with L = 400 and N = 4. The spectral efficiency measures the amount of data that can be transmitted per unit of bandwidth. when 20% of UEs are considered, the LPMMSE technique achieves a spectral efficiency of 8.9537bit/s/Hz, the PRZF technique achieves 10.975bit/s/Hz, the PMMSE technique achieves 11.0135bit/s/Hz, and the Proposed technique achieves the highest spectral efficiency of 20.331bit/s/Hz.

Overall, the table demonstrates that the Proposed method provides superior downlink spectral efficiency per UE compared to the LPMMSE, PRZF, and PMMSE techniques in the given scenario. This suggests that the Proposed method is more effective in maximizing data transmission rates and utilizing the available bandwidth efficiently for a range of UE percentages.

4.1.2. Performance comparrision of proposed precoding scheme with Scalable precoding based on Sum SE

Figure 4.5 presents a comparison of the sum downlink spectral efficiency per user equipment (UE) for different precoding techniques in a specific scenario. The scenario involves a 1 km2 area with L = 400 and N = 1. The spectral efficiency measures the total data that can be transmitted in the downlink direction per unit of bandwidth. The figure shows the sum spectral efficiency values for the proposed method and other centralized and distributed precoding techniques. The purpose of the comparison is to assess the effectiveness of the proposed method in maximizing the overall spectral efficiency in the downlink. By comparing it with other techniques, we can determine whether the proposed method provides better performance. The advantage of accommodating more user equipment (UEs) simultaneously is that the total spectral efficiency (SE) experiences an almost linear growth with the increase in the number of UEs, as depicted in Figure 4.5. This observation demonstrates the capability of a cell-free network to serve a large quantity of UEs effectively.

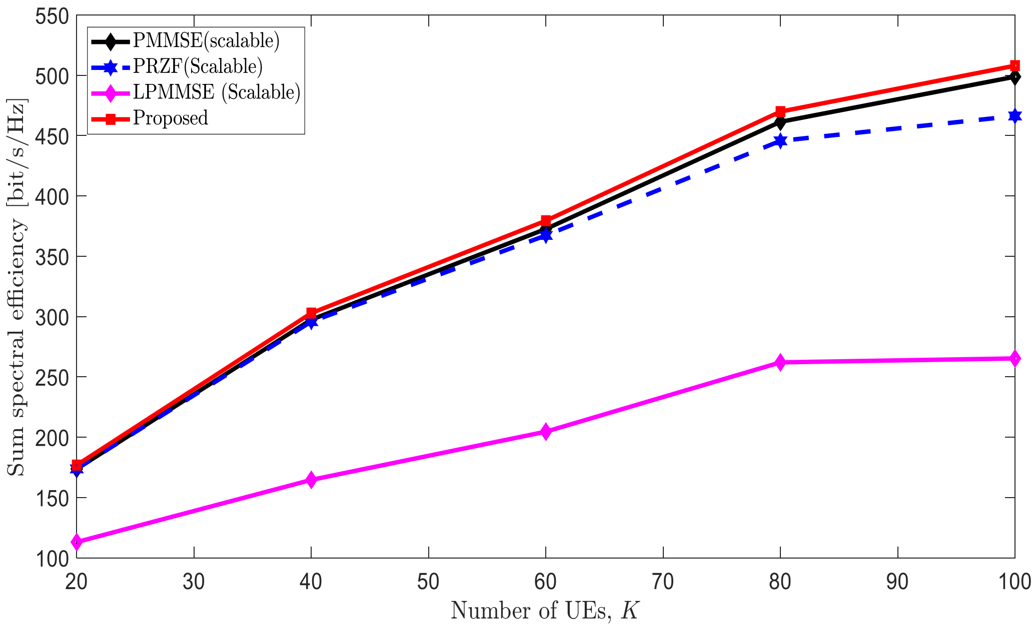

Figure 4. 5. Sum DL SE per UE with different scalable and proposed precoding schemes at L=400 and N=1 in a 1km^2 region.

When we considered 20% of UEs, the LPMMSE technique achieves a sum spectral efficiency of 110.987bit/s/Hz, the PRZF technique achieves 170.219bit/s/Hz, the PMMSE technique achieves 170.421bit/s/Hz, and the Proposed method achieves the highest sum spectral efficiency of 174.788bit/s/Hz. Overall, the figure provides a visual representation of how the proposed method performs in terms of sum downlink spectral efficiency per UE when compared to other precoding techniques. The results will help in understanding the relative merits and performance of the proposed method and its potential advantages in the given scenario.

Table 4. 6: Sum DL SE per UE with different scalable and proposed precoding schemes at L=400 and N=1 in a 1km^2 region for different number of UEs.

Sum DL SE per user equipment (UE)					
S.No	No. UE	LPMMSE	PRZF	PMMSE	Poposed
1	20	110.987	170.219	170.421	174.788
2	40	151.2675	290.4964	296.4513	306.4962
3	60	220.7643	365.567	370.9462	386.2672
4	80	252.9746	446.764	472.8642	476.2674
5	100	267.954	469.259	499.006	508.145

Table 4.6 provides a comparative analysis of the sum DL SE per user equipment (UE) for different precoding techniques in a specific scenario. The scenario involves a 1 km2 area with L = 400 and N = 1. The sum SE quantifies the overall data transmission capacity in the downlink direction per unit of bandwidth, considering all user equipment (UE) in the system. The table offers valuable information regarding the performance of the proposed method in comparison to existing scalable precoding techniques. It illustrates that the proposed method significantly improves the overall downlink spectral efficiency per UE, indicating its potential as an effective approach for maximizing data transmission rates and efficiently utilizing the available bandwidth in the specified scenario.

Figure 4.6 presents a graphical representation of the comparison between the sum DL SE per user equipment (UE) for the proposed method and other scalable precoding techniques. The assessment is carried out in a specific scenario, involving a 1 km2 area with L = 400 and N = 2. The purpose of the figure is to visually demonstrate the performance of the proposed method in terms of sum DL SE compared to other precoding techniques. By comparing it with alternative methods, we can evaluate whether the proposed method exhibits superior performance.

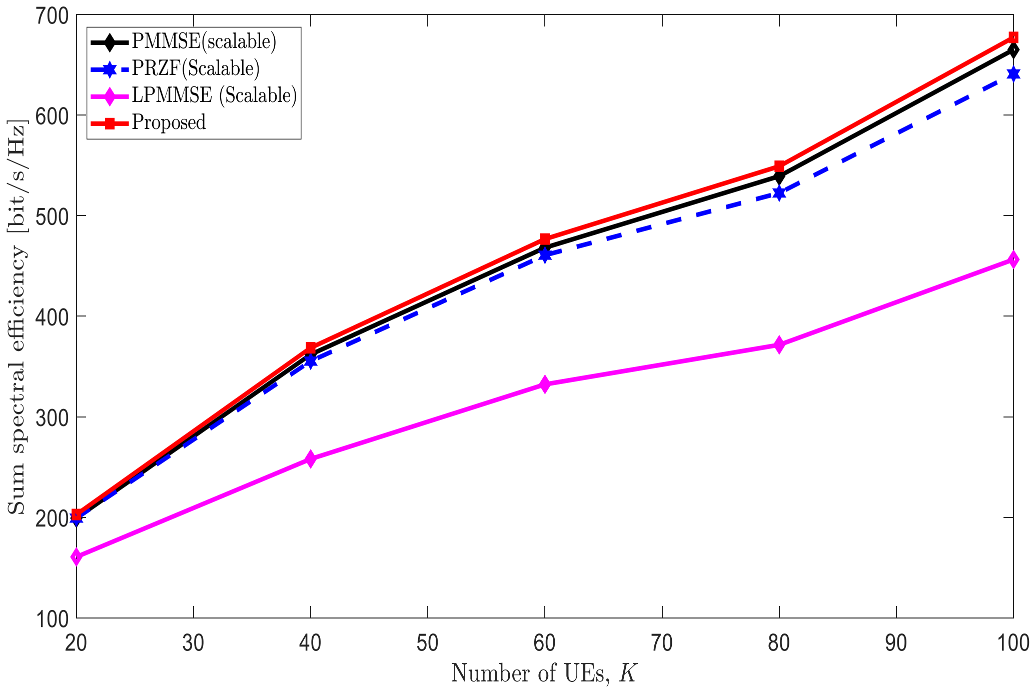

Figure 4. 6. Sum DL SE per UE with different scalable and proposed precoding schemes at L=400 and N=2 in a 1km^2 region for different number of UEs.

The figure provides a clear visual representation of how the proposed method performs in terms of sum downlink spectral efficiency per UE when compared to other precoding techniques. The results obtained from this comparison can provide insights into the relative merits and performance of the proposed method, indicating its potential advantages in the given scenario. This indicates that when there are 100 UEs in the system, the proposed method outperforms the other techniques, providing the highest spectral efficiency per UE. It implies that the proposed method can transmit more data per unit of bandwidth for each individual UE compared to the other techniques in the given scenario.

Table 4. 7: Sum DL SE per UE with different scalable and proposed precoding schemes at L=400 and N=2 in a 1km^2 region for different number of UEs.

Sum downlink spectral efficiency per user equipment (UE)					
S.No	No.UE	LPMMSE	PRZF	PMMSE	Proposed
1	20	147.597	194.908	195.908	198.666
2	40	256.2431	339.2601	345.268	356.286
3	60	336.4235	442.047	451.981	461.8012
4	80	348.1067	529.467	553.967	567.672
5	100	443.873	612.001	637.823	649.505

Table 4.7 provides a comparative analysis of the sum downlink spectral efficiency per user equipment (UE) for different precoding techniques in a specific scenario. The scenario involves a 1 km2 area with L = 400 and N = 2. The sum spectral efficiency represents the total amount of data that can be transmitted in the downlink direction per unit of bandwidth, considering all UEs in the system. For instance, when 20% of UEs are considered, the LPMMSE technique achieves a sum spectral efficiency of 147.597 bit/s/Hz, the PRZF technique achieves 194.908 bit/s/Hz, the PMMSE technique achieves 195.908 bit/s/Hz, and the proposed method achieves the highest sum spectral efficiency of 198.666bit/s/Hz. The table provides valuable insights into the performance of the proposed method compared to existing centralized and distributed precoding techniques. It demonstrates that the Proposed method offers enhanced overall downlink spectral efficiency per UE, making it a promising approach for maximizing data transmission rates and utilizing the available bandwidth efficiently in the given scenario.

Figure 4.7 illustrates the comparison between the sum downlink spectral efficiency per user equipment (UE) for different precoding techniques in a specific scenario. The scenario involves a 1 km2 area with L = 400 and N = 3. The sum spectral efficiency represents the total amount of data that can be transmitted in the downlink direction per unit of bandwidth, taking into account all UEs in the system.

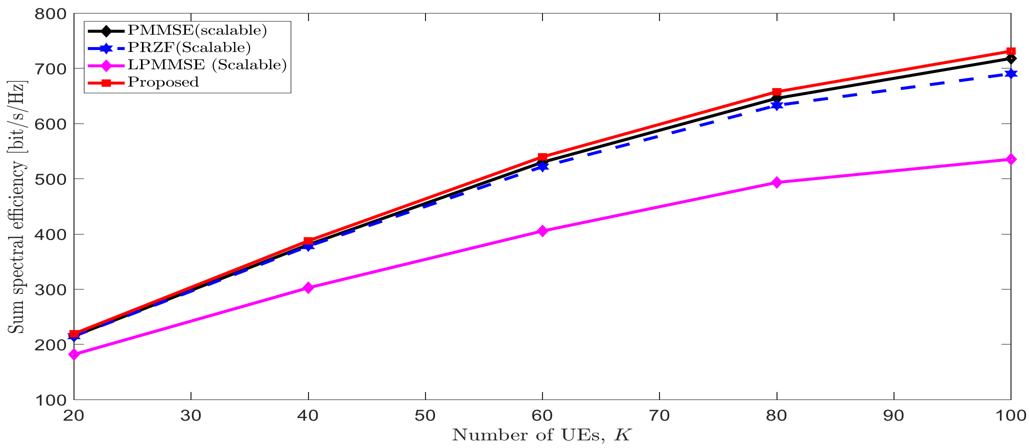

Figure 4. 7. Sum DL SE per UE with different scalable and proposed precoding schemes at L=400 and N=3 in a 1km^2 region for different number of UEs.

For instance, when there are 20 UEs in the system, the LPMMSE technique achieves a sum SE of 182.049bit/s/Hz, the PRZF technique achieves 216.415bit/s/Hz, the PMMSE technique achieves 217.049bit/s/Hz, and the proposed method achieves the highest sum spectral efficiency of 219.455bit/s/Hz. While UE=100, the LPMMSE technique achieves an SE of 535.5147 bit/s/Hz, the PRZF technique achieves 690.443 bit/s/Hz, the PMMSE technique achieves 718.118 bit/s/Hz, and the Proposed method achieves the highest SE of 731.272 bit/s/Hz. This indicates that when there are 100 UEs in the desired system, the proposed method outperforms the other techniques, providing the highest SE per UE.

Table 4. 8: Sum DL SE per UE with different scalable and proposed precoding schemes at L=400 and N=3 in a 1km^2 region for different number of UEs.

Sum downlink spectral efficiency per user equipment (UE)					
S.No	No.UE	LPMMSE	PRZF	PMMSE	Proposed
1	20	182.049	216.415	217.049	219.455
2	40	295.452	386.267	387.9672	395.3466
3	60	397.346	524.7612	526.874	546.675
4	80	519.467	659.489	663.76	686.657
5	100	535.5147	690.443	718.118	731.272

Table 4.8 presents a comparative analysis of the sum downlink SE per user equipment (UE) for different precoding techniques in a specific scenario. The scenario involves a 1 km2 area with L = 400 and N = 3. The sum spectral efficiency represents the overall data that can be transmitted in the downlink direction per unit of bandwidth, considering all UEs in the system. For instance, when there are 20 UEs in the system, the LPMMSE technique achieves a sum spectral efficiency of 182.049bit/s/Hz, the PRZF technique achieves 216.415bit/s/Hz, the PMMSE technique achieves 217.049bit/s/Hz, and the proposed method achieves the highest sum spectral efficiency of 219.455bit/s/Hz.

The table provides valuable insights into the SE achieved by the proposed method and other precoding techniques, highlighting the potential advantages and performance of the proposed method in maximizing downlink data transmission rates per UE at different UE densities.

Figure 4.8 presents a graphical representation that compares the sum DL SEper user equipment achieved by the proposed method with other scalable precoding techniques. This analysis was performed within a specified 1 km2 area, considering a system configuration with L = 400 and N = 4. The figure visually shows the performance of different precoding techniques in terms of the total amount of data that can be transmitted in the downlink direction per unit of bandwidth, considering all UEs in the system.

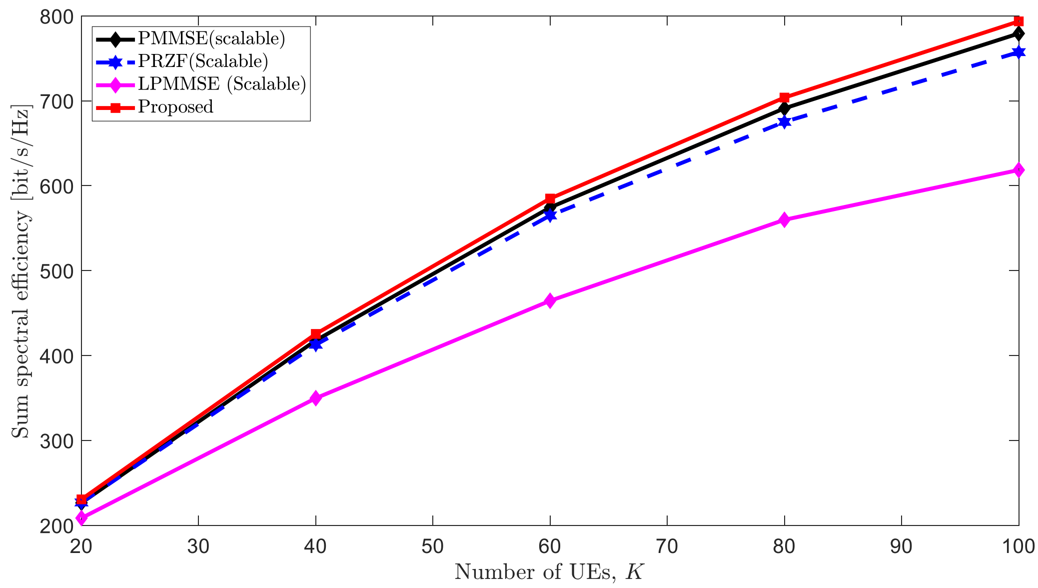

Figure 4. 8. Sum DL SE per UE with different scalable and proposed precoding schemes at L=400 and N=4 in a 1km^2 region for different number of UEs.

The figure provides spectral efficiency values for four precoding techniques: LPMMSE, PRZF, PMMSE, and the proposed method. These values represent the amount of data that can be transmitted in the downlink direction per unit of bandwidth, considering all UEs in the system. For instance, when there are 20 UEs in the system, the LPMMSE technique achieves a sum spectral efficiency of 203.31bit/s/Hz, the PRZF technique achieves 218.5bit/s/Hz, the PMMSE technique achieves 219.5701bit/s/Hz, and the proposed method achieves the highest sum spectral efficiency of 224.305bit/s/Hz.

Table 4. 9: Sum DL SE per UE with different scalable and proposed precoding schemes at L=400 and N=4 in a 1km^2 region for different number of UEs.

Sum downlink spectral efficiency per user equipment (UE)					
S.No	No.UE	LPMMSE	PRZF	PMMSE	Proposed
1	20	203.31	218.5	219.5701	224.305
2	40	346.267	396.7642	398.5786	405.2563
3	60	436.689	536.6721	542.654	556.76
4	80	556.746	676.761	687.664	702.4678
5	100	642.192	794.359	820.623	835.652

Table 4.9 displays and compares the sum downlink spectral efficiency achieved per user equipment (UE) for different precoding techniques. The analysis is performed in a 1 km2 area, utilizing a system configuration with L = 400 and N = 4.

The table provides spectral efficiency values for four precoding techniques: LPMMSE, PRZF, PMMSE, and the proposed method. These values represent the amount of data that can be transmitted in the downlink direction per unit of bandwidth, considering all UEs in the system. For instance, when there are 20 UEs in the system, the LPMMSE technique achieves a sum spectral efficiency of 203.31bit/s/Hz, the PRZF technique achieves 218.5bit/s/Hz, the PMMSE technique achieves 219.5701bit/s/Hz, and the Proposed method achieves the highest sum spectral efficiency of 224.305bit/s/Hz. Table 4.9 serves as an informative resource, summarizing the spectral efficiency achieved by the proposed method and alternative precoding techniques. It allows stakeholders to understand and compare the capabilities of different techniques, facilitating the identification of the most effective approach for achieving optimal downlink spectral efficiency per UE.

4.1.3. Performance comparrision of Scalable precoding with the Existing precoding based on CDF and Spectral efficiency

The evaluation focuses on two metrics: Cumulative Distribution Function (CDF) and Spectral Efficiency. The CDF metric offers an understanding of overall system performance by examining the distribution of key performance indicators. Spectral Efficiency measures the effectiveness of data transmission per unit of bandwidth. The purpose of the comparison is to determine if scalable precoding outperforms existing techniques in terms of these metrics. The results demonstrate the improvements achieved by scalable precoding in terms of enhanced CDF and increased spectral efficiency. The CDF analysis reveals that scalable precoding surpasses existing techniques in achieving higher performance indicators throughout the system. The comparison of Spectral Efficiency indicates that scalable precoding enables more efficient data transmission, resulting in higher data rates per unit of bandwidth. These findings emphasize the potential advantages of scalable precoding in enhancing system performance and data transmission efficiency.

Figure 4.9 illustrates the CDF of the downlink spectral efficiency per user equipment (UE) for different precoding techniques. The proposed method is compared to both centralized and distributed precoding techniques. The analysis is performed using a system configuration with L = 400 and N = 1, covering a 1 km2 area.

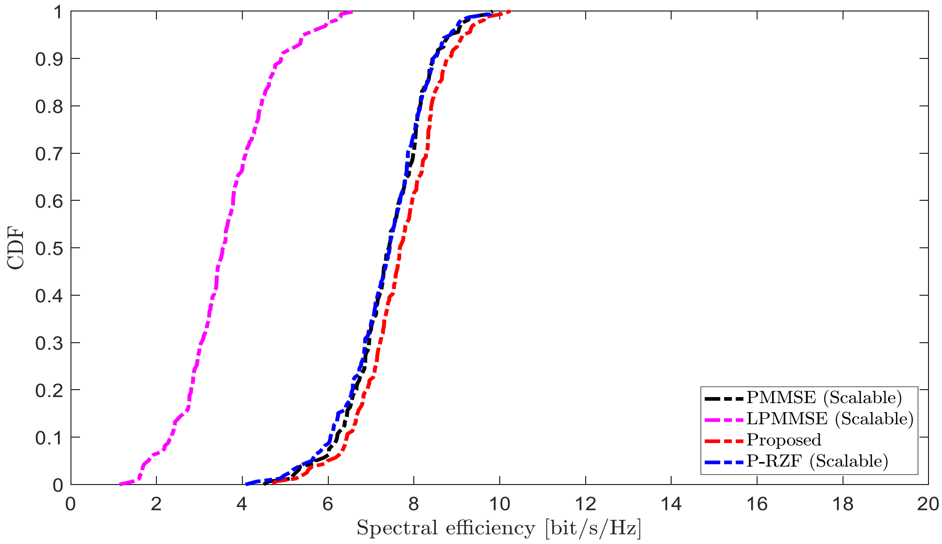

Figure 4. 9. DL SE per UEs for the proposed method and different scalable precoding schemes at L = 400, N = 1 and k=100 in a 1 km^2 area.

When the CDF level is set at 0.2, the LPMMSE technique achieves a spectral efficiency value of 2.7696 bit/s/Hz, the PRZF technique achieves a value of 6.5456 bit/s/Hz, the PMMSE technique achieves a value of 6.683 bit/s/Hz, and the proposed method achieves a value of 6.9573 bit/s/Hz. Furthermore, the proposed method demonstrates superior performance compared to LPMMSE, PRZF, and PMMSE techniques at each CDF level. This indicates that the proposed method consistently provides higher downlink spectral efficiency per UE, resulting in more efficient data transmission.

Table 4. 10: DL SE per UEs for the proposed method and different scalable precoding schemes at L = 400, N = 1 and k=100 in a 1 km^2 area.

Spectral efficiency per UEs based on CDF value (bit/s/Hz)					
S.No	CDF	LPMMSE	PRZF	PMMSE	Proposed
1	0.2	2.7696	6.5456	6.683	6.9573
2	0.4	3.343	7.0745	7.1153	7.5053
3	0.6	3.784	7.6938	7.7475	8.003
4	0.8	4.4523	8.1134	8.28	8.651
5	1	6.6475	9.7823	9.7916	10.2488

Table 4.10 displays and compares the CDF values of the downlink spectral efficiency per user equipment (UE) for different precoding techniques. The comparison is made between the proposed method, as well as scalable precoding techniques. The analysis is performed using a system configuration with L = 400 and N = 1, covering a 1 km2 area. The table

presents the CDF values for different levels of DL SE per UE, ranging from 0.2 to 1.0. Each precoding technique, namely LPMMSE, PRZF, PMMSE, and the proposed method, is associated with specific CDF values at these efficiency levels. For instance, at a CDF level of 0.2, the value of SE for the LPMMSE technique is 2.7696bit/s/Hz, for the PRZF technique it is 6.5456bit/s/Hz, for the PMMSE technique it is 6.683, and for the proposed method it is 6.9573bit/s/Hz. These results emphasize the effectiveness of the proposed method in optimizing spectral efficiency and addressing the increasing demands for high-quality data transmission. The superior performance of the proposed method across different CDF levels showcases its ability to deliver reliable and high-speed communication services.

Figure 4.10 presents the Cumulative Distribution Function (CDF) of the downlink spectral efficiency per user equipment (UE) for the proposed method, along with other centralized and distributed precoding techniques. The figure specifically compares the performance of these techniques under the system parameters L = 400, N = 2, and K = 100.

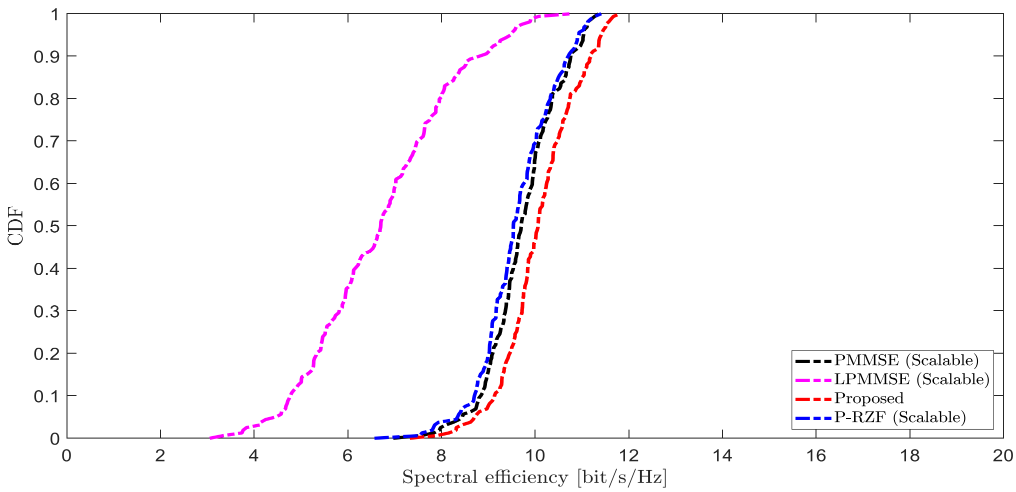

Figure 4. 10. DL SE per UEs for the proposed method and different scalable precoding schemes at L = 400, N = 2 and k=100 in a 1 km^2 area.

For every CDF level, the table presents the respective spectral efficiency values per user equipment (UE) for each technique. For example, at a CDF level of 0.2, the LPMMSE technique achieves a spectral efficiency of 4.3032 bit/s/Hz, whereas the PRZF technique achieves 8.0788 bit/s/Hz, the PMMSE technique achieves 8.2989 bit/s/Hz, and the proposed method achieves 8.566 bit/s/Hz.

Table 4. 11: DL SE per UEs for the proposed method and different scalable precoding schemes at L = 400, N = 2 and k=100 in a 1 km^2 area.

Spectral efficiency per UEs based on CDF value (bit/s/Hz)					
S.No	CDF	LPMMSE	PRZF	PMMSE	Proposed
1	0.2	4.3032	8.0788	8.2989	8.566
2	0.4	5.1966	8.4972	8.7286	8.9978
3	0.6	5.5998	8.9676	9.1985	9.3817
4	0.8	6.7955	9.5113	10.0432	9.5949
5	1	10.7373	11.437	11.7256	11.9692

Table 4.11 presents a comparison of the Cumulative Distribution Function (CDF) of the downlink spectral efficiency per user equipment (UE) for the proposed method and other centralized and distributed precoding techniques. The table specifically focuses on the system parameters L = 400, N = 2, and K = 100. At each CDF level, the corresponding values of spectral efficiency per UEs for each technique are provided in the table. For instance, at a CDF level of 0.2, the LPMMSE technique achieves a spectral efficiency of 4.3032bit/s/Hz, while the PRZF technique achieves 8.0788bit/s/Hz, the PMMSE technique achieves 8.2989bit/s/Hz, and the proposed method achieves 8.566bit/s/Hz.

Figure 4.11 compares the Cumulative Distribution Function (CDF) of downlink spectral efficiency (UE) for the proposed method with other scalable precoding techniques. The comparison is conducted under specific system parameters: L = 400, N = 3 and K = 100. The figure provides a graphical representation of the CDF curves, which depict the probability distribution of achieving different spectral efficiency values for each precoding technique. By analyzing the curves, we can assess how the proposed method performs in comparison to the other techniques in terms of downlink spectral efficiency per UE.

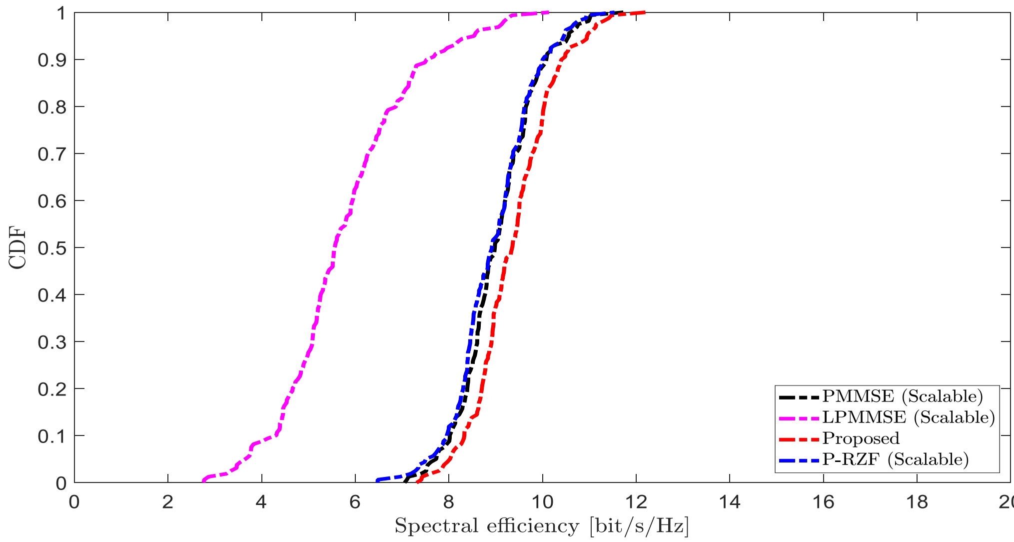

Figure 4. 11. DL SE per UEs for the proposed method and different scalable precoding schemes at L = 400, N = 3 and k=100 in a 1 km^2 area.

For each CDF level, the table showcases the respective spectral efficiency values per UEs achieved by each technique. For example, at a CDF level of 0.2, the LPMMSE technique attains a spectral efficiency of 4.6032 bit/s/Hz, while the PRZF technique reaches 8.188 bit/s/Hz, the PMMSE technique records 8.3289 bit/s/Hz, and the proposed method achieves 8.66bit/s/Hz.

Table 4. 12: DL SE per UEs for the proposed method and different scalable precoding schemes at L = 400, N = 3 and k=100 in a 1 km^2 area.

Spectral efficiency per UEs based on CDF value (bit/s/Hz)					
S.No	CDF	LPMMSE	PRZF	PMMSE	Proposed
	0.2	4.6032	8.188	8.3289	8.66
	0.4	5.3066	8.5972	8.7286	9.0781
	0.6	5.8998	9.0765	9.185	9.4817
	0.8	6.8955	9.594	10.0432	9.7113
	1	10.1373	11.537	11.7256	12.3969

Table 4.12 presents a contrast between the Cumulative Distribution Function (CDF) of the downlink spectral efficiency per user equipment (UE) for the proposed method and alternative scalable precoding techniques. The emphasis of the table is on specific system

parameters: L = 400, N = 3 and K = 100. The table displays the spectral efficiency values per UEs at different CDF levels, spanning from 0.2 to 1.0. Four precoding techniques, namely LPMMSE, PRZF, PMMSE, and the proposed method, are subjected to comparison. For each CDF level, the table showcases the respective spectral efficiency values per UEs achieved by each technique. For example, at a CDF level of 0.2, the LPMMSE technique attains a spectral efficiency of 4.6032 bit/s/Hz, while the PRZF technique reaches 8.188 bit/s/Hz, the PMMSE technique records 8.3289 bit/s/Hz, and the proposed method achieves 8.66bit/s/Hz.

Figure 4.12 shows a cumulative distribution function (CDF) that compares the downlink spectral efficiency per user equipment (UE) for the proposed method with other scalable precoding techniques. The CDF provides information about the probability distribution of spectral efficiency among various UE devices. It illustrates how the proposed technique performs in terms of downlink spectral efficiency when compared to other methods. SE denotes the quantity of data that can be transmitted over a specific bandwidth.

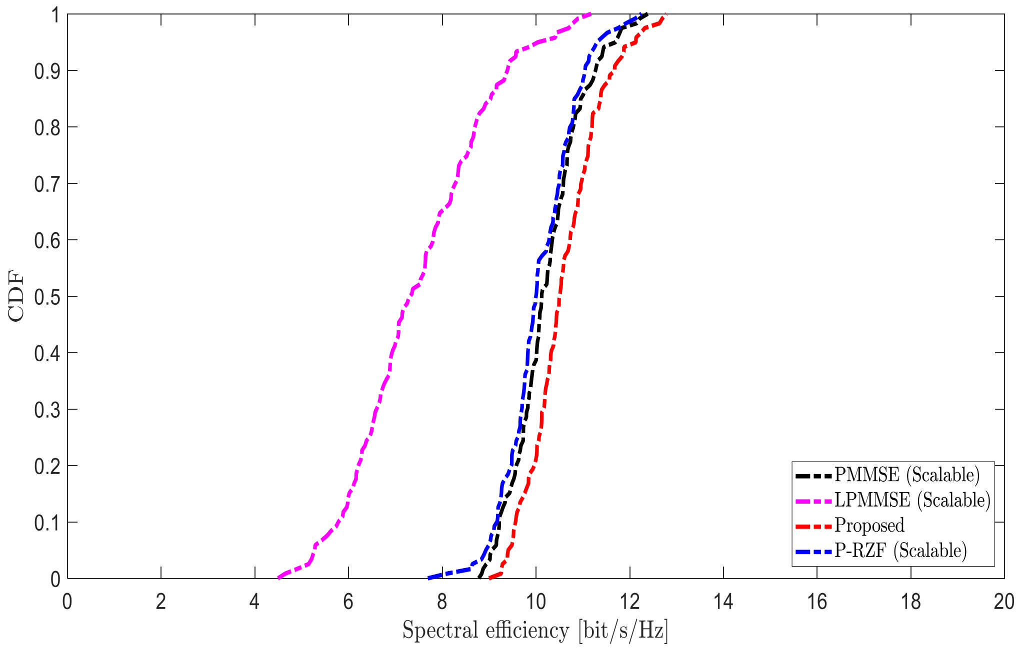

Figure 4. 12. DL SE per UEs for the proposed method and different scalable precoding schemes at L = 400, N = 4 and k=100 in a 1 km^2 area.

At CDF of 0.2, the spectral efficiency values for the different techniques are as follows: PMMSE 5.6132bit/s/Hz PRZF 8.788 bit/s/Hz, MMSE 8.9289bit/s/Hz, proposed 9.2646bit/s/Hz. These values indicate that at the 20th percentile of the distribution, the proposed method achieves the highest spectral efficiency per UE with a value of 9.2646bit/s/Hz. It outperforms LPMMSE, PRZF, and PMMSE, which have spectral efficiency values of 5.6132bit/s/Hz, 8.788bit/s/Hz, and 8.9289bit/s/Hz, respectively. At CDF = 1, representing the maximum value in the distribution, the spectral efficiency values for the different techniques are: LPMMSE = 11.6373bit/s/Hz, PRZF = 12.1937 bit/s/Hz, PMMSE = 12.2256 bit/s/Hz, proposed = 12.6969 bit/s/Hz. In this case, the proposed method still exhibits the highest spectral efficiency per UE with a value of 12.6969 bit/s/Hz. LPMMSE, PRZF, and PMMSE achieve spectral efficiency values of 11.6373 bit/s/Hz, 12.1937 bit/s/Hz and 12.2256 bit/s/Hz respectively. These findings highlight the effectiveness of the proposed method in maximizing the overall spectral efficiency in the downlink. The results provide valuable insights into the relative merits and performance of different precoding techniques, reaffirming the potential advantages of the proposed method for enhancing data transmission rates and efficient utilization of the available bandwidth.

Table 4. 13: DL SE per UEs for the proposed method and different scalable precoding schemes at L = 400, N = 4 and k=100 in a 1 km^2 area.

Spectral efficiency per UEs based on CDF value (bit/s/Hz)					
S.No	CDF	LPMMSE	PRZF	PMMSE	Proposed
1	0.2	5.6132	8.788	8.9289	9.2646
2	0.4	6.3076	9.5972	9.7286	10.0781
3	0.6	7.9898	10.0765	10.185	10.4817
4	0.8	8.9965	11.0945	11.1432	11.3813
5	1	11.6373	12.1937	12.2256	12.6969

Table 4.13 presents a comparison of the cumulative distribution function (CDF) of the downlink spectral efficiency per user equipment (UE) for the proposed method in comparison to other centralized and distributed precoding techniques. The evaluation is conducted at specific parameter settings: L = 400, N = 4, and K = 100. The table consists of several entries with corresponding CDF values and spectral efficiency values for each technique. The different techniques being compared are LPMMSE, PRZF, PMMSE, and the Proposed method. In summary, Table 4.13 provides a concise representation of the CDF of the downlink spectral efficiency per UE for different precoding techniques. The data in the table demonstrates the superiority of the Proposed method in terms of achieving higher spectral efficiency values, indicating its potential advantages in maximizing data transmission rates and utilizing the available bandwidth efficiently.

4.1.4. Performance comparision of Proposed Method (Precoding) with Scalable precoding based on BER and SNR valus.

In this research, our objective is to assess and emphasis the effectiveness of Scalable Precoding in comparison to established precoding techniques through an examination of BER and SNR values. Precoding holds a critical role in wireless communication systems as it optimizes signal transmission to enhance overall system performance. By conducting a comprehensive performance analysis, we can acquire valuable insights into the efficacy and potential benefits of Scalable Precoding over traditional approaches. This investigation will contribute to the ongoing research efforts aimed at enhancing wireless communication systems and facilitating the development of more efficient precoding techniques.

- **Bit Error Rate (BER):** BER is a fundamental metric that measures the rate of errors in digital data transmission in cell-free massive MIMO systems. It is influenced by the signal-to-noise ratio (SNR) and the QAM modulation order used.
- **Signal-to-Noise Ratio (SNR):** SNR is a measure of the desired signal strength relative to the background noise level in cell-free massive MIMO. It is affected by factors like transmit power, number of access points, channel conditions, and receiver noise. The required SNR to achieve a target BER depends on the QAM modulation order, with higher-order QAM needing a higher SNR.
- **BER-SNR Relationship in Cell-Free Massive MIMO**: There is a trade-off between BER and SNR in cell-free massive MIMO with QAM. Considering factors like access point count and receiver processing. Analyzing the BER-SNR relationship allows system designers to optimize parameters like transmit power, access point count, and QAM order to balance BER and spectral efficiency.

Figure 4.13 presents a comparison of the performance in terms of BER between a proposed method and various centralized and distributed precoding techniques. The comparison is conducted under specific conditions: L = 400, N = 1 and K = 100. The table displays the BER values for different precoding techniques, which are evaluated based on SNR values given in decibels (dB).

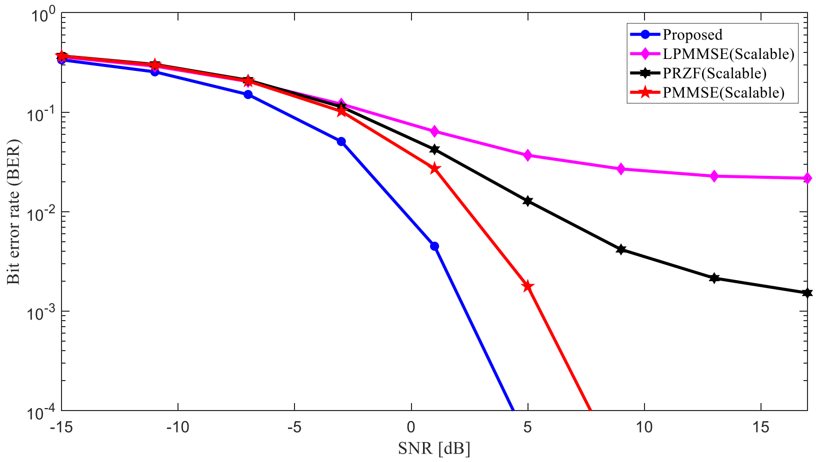

Figure 4. 13. BER of proposed method and other scalable precoding techniques at L = 400 and N = 1, and K=100 with different SNR values.

For instance, at an SNR of -15dB, the LPMMSE technique results in a BER of 0.36602, PRZF achieves a BER of 0.36402, PMMSE achieves a BER of 0.3592, and the proposed method achieves a BER of 0.336. At an SNR of 10dB, the BER values for each precoding technique: LPMMSE = 0.0269 PRZF = 0.00417, PMMSE Approximately 0.0001 and the Proposed method Approximately 0.0001 bit error values. These values indicate the error rates achieved by each precoding technique at the specified SNR level. A lower BER value indicates better performance, as it signifies a lower occurrence of errors during transmission. For instance, the LPMMSE technique achieves a BER of 0.0269, indicating that approximately 2.69% of the transmitted bits experience errors. The PRZF technique demonstrates superior performance with a BER of 0.00417, representing an error rate of approximately 0.417%. Both the PMMSE technique and the proposed method exhibit similar performance, with BER values approximately equal to 0.0001 or 0.01%.

Table 4. 14: BER of proposed method and other scalable precoding techniques at L = 400 and N = 1, and K=100 with different SNR values.

Bit Error Rate of Precoding techniques based on SNR values (dB)					
S.No	SNR(dB)	LPMMSE	PRZF	PMMSE	Proposed
1	-15dB	0.36602	0.36402	0.3592	0.336
2	-10dB	0.30227	0.2982	0.29017	0.2544
3	-5dB	0.12065	0.1133	0.1021	0.05077
4	0dB	0.0642	0.04225	0.027	0.0045
5	5dB	0.0369	0.0128	0.00177	$\approx 10^{-4}$
6	10dB	0.0269	0.00417	$\approx 10^{-4}$	$\approx 10^{-4}$

Table 4.14 compares the performance of scalableprecoding techniques, including a proposed method, centralized precoding, and distributed precoding, in terms of Bit Error Rate (BER). The comparison is conducted using Signal-to-Noise Ratio (SNR) values in decibels (dB) as the measurement. By analyzing the BER values across different SNR levels, it is possible to evaluate the performance of each precoding technique. The table facilitates the assessment of the proposed method in comparison to centralized and distributed precoding techniques, allowing for insights into their relative performance under specific conditions. In essence, Figure 4.14 presents a graphical comparison of the BER performance between the proposed method and other centralized and distributed precoding techniques. It provides insights into the performance of these techniques in terms of error rate under specific parameter settings of L = 400, N = 2, and K = 100.

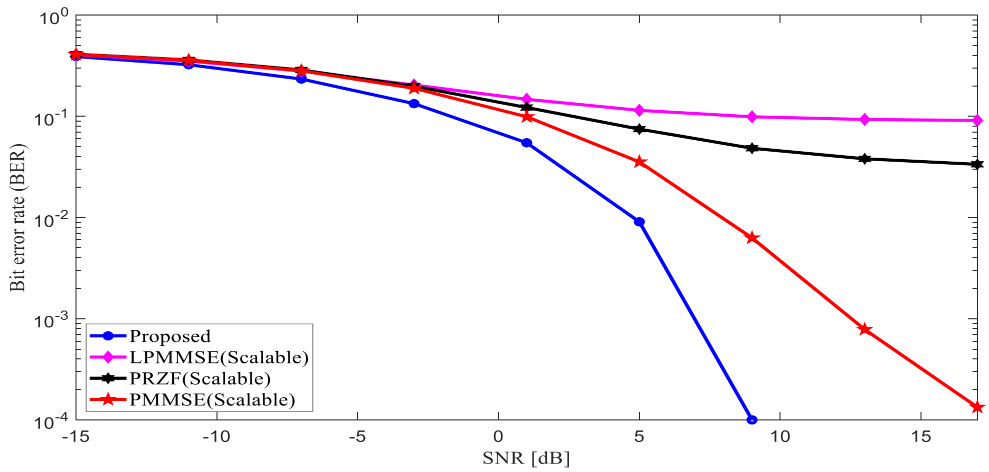

Figure 4. 14. BER of proposed method and other scalable precoding techniques at L = 400 and N = 2, and K=100 with different SNR values.

For instance, at an SNR of -15dB, figure 4.14 shows that LPMMSE, PRZF, PMMSE, and the proposed method achieve BER values of 0.4119, 0.4112, 0.4098, and 0.3895, respectively. The figure also shows BER values for each technique at other SNR levels ranging from -15dB to 10dB. The proposed method achieves the lowest BER value at 10 dB, indicating the best performance in terms of error correction, PRZF also exhibits good performance with a BER value of 0.048366, LPMMSE has a higher BER value of 0.09898 compared to the proposed method and PRZF, and PMMSE achieves a BER value of 0.00628, which is higher than the proposed method but lower than PRZF and LPMMSE.

Table 4. 15: BER of proposed method and other scalable precoding techniques at L = 400 and N = 2, and K=100 with different SNR values.

Bit Error Rate of Precoding techniques based on SNR values (dB)					
S.No	SNR(dB)	LPMMSE	PRZF	PMMSE	Proposed
1	-15dB	0.4119	0.4112	0.4098	0.3895
2	-10dB	0.28708	0.28708	0.2816	0.23366
3	-5dB	0.20403	0.19865	0.1892	0.13358
4	0dB	0.1474	0.12228	0.09908	0.5478
5	5dB	0.1146	0.07476	0.03543	0.009066
6	10dB	0.09898	0.048366	0.00628	$\approx 10^{-4}$

Table 4.15 compares the performance of different precoding techniques in terms of Bit Error Rate (BER). The focus is specifically on the parameter values of L = 400, N = 2, and K = 100. These values indicate the BER achieved by each technique at an SNR level of 10dB. Lower BER values represent better performance, as they indicate a reduced rate of errors during transmission. In this case, the proposed method exhibits the lowest BER value, implying superior error correction capabilities and a higher level of accuracy in data transmission at an SNR of 10dB.

Figure 4.15 presents a comparison of the Bit Error Rate (BER) performance between the proposed method and other centralized and distributed precoding techniques. The specific parameter values used for this comparison are L = 400, N = 3, and K = 100. For each SNR level, figure 4.15 shows the corresponding BER values for each technique. Lower BER values indicate better performance in terms of reducing errors during transmission. When SNR value of -15dB, the figure shows that LPMMSE, PRZF, PMMSE, and the proposed method achieve BER values of 0.43443, 0.43443, 0.43341, and 0.40882, respectively. Similarly, the figure provides the BER values for each technique at other SNR levels ranging from -15dB to 10dB.

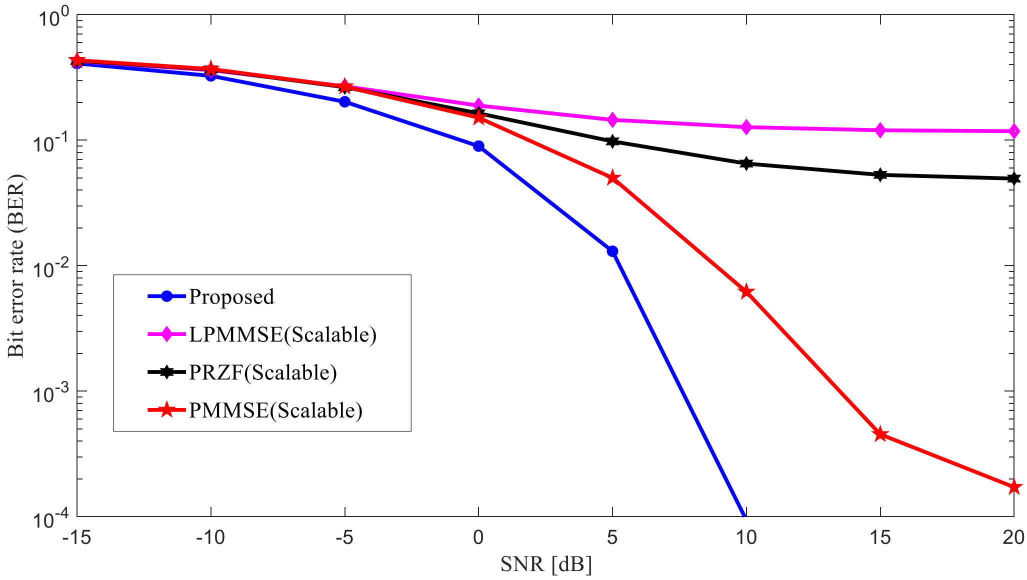

Figure 4. 15. BER of proposed method and other scalable precoding techniques at L = 400 and N = 3, and K=100 with different SNR values.

Through an analysis of the BER values across various Signal-to-Noise Ratio (SNR) levels, it becomes apparent that the proposed method consistently outperforms the other techniques. It achieves lower BER values, indicating superior error correction capabilities and a reduced occurrence of transmission errors. Across SNR levels ranging from -15dB to 10dB, the proposed method consistently demonstrates lower BER values compared to LPMMSE, PRZF, and PMMSE.

Table 4. 16: BER of proposed method and other scalable precoding techniques at L = 400 and N = 3, and K=100 with different SNR values.

Bit Error Rate of Precoding techniques based on SNR values (dB)					
S.No	SNR(dB)	LPMMSE	PRZF	PMMSE	Proposed
1	-15dB	0.43443	0.43443	0.43341	0.40882
2	-10dB	0.36937	0.3669	0.3618	0.3257
3	-5dB	0.26879	0.26706	0.2643	0.2024
4	0dB	0.18875	0.16379	0.151219	0.08971
5	5dB	0.1452	0.0978	0.050046	0.01303
6	10dB	0.127047	0.06514	0.006514	$\approx 10^{-4}$

Table 4.16 provides a comparison of the Bit Error Rate (BER) performance between the proposed method and other centralized and distributed precoding techniques. The table

specifically focuses on the parameter values of L = 400, N = 3, and K = 100. Overall, the table facilitates a comparison of the BER performance among different precoding techniques, considering the specified parameter settings. It offers valuable insights into how the proposed method performs relative to other techniques at various SNR levels, enabling evaluation and comprehension of their respective error-correction capabilities during data transmission.

Figure 4.16 presents a graphical comparison of the performance of the proposed method and various centralized and distributed precoding techniques in terms of Bit Error Rate (BER). The figure specifically highlights the parameter settings of L = 400, N = 4, and K = 100.

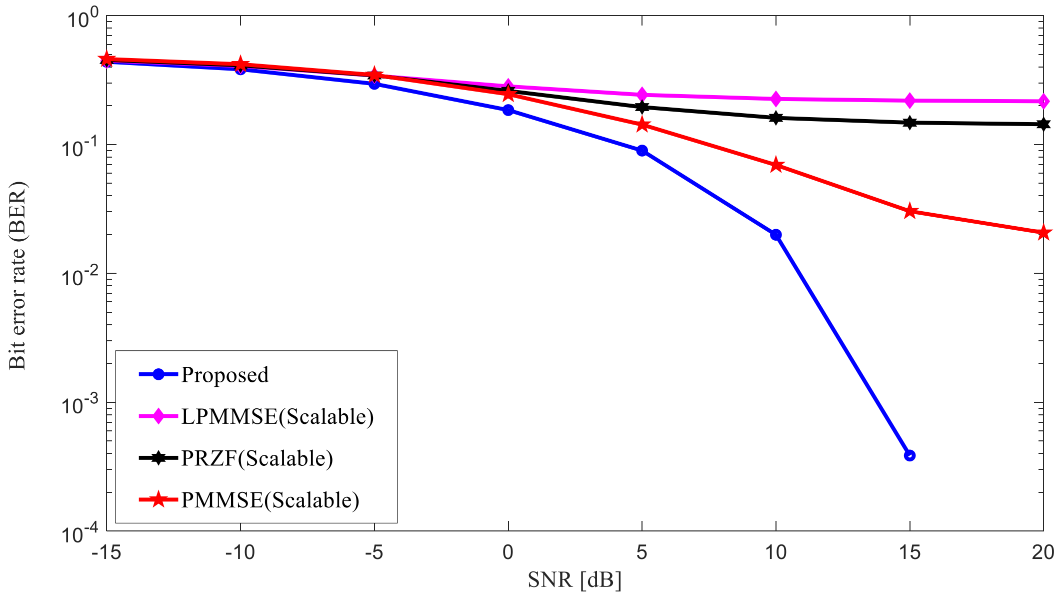

Figure 4. 16. BER of proposed method and other scalable precoding techniques at L = 400 and N = 4, and K=100 with different SNR values.

For instance, the BER values for LPMMSE, PRZF, PMMSE, and the proposed method are 0.44105, 0.44105, 0.43355, and 0.4212, respectively, at -15 dB SNR. As the Signal-to-Noise Ratio (SNR) increases, all precoding techniques demonstrate improved BER performance. However, the proposed method consistently exhibits the most favorable BER values, suggesting its superiority across different SNR conditions. The performance gap between the proposed method and the other techniques widens as the SNR increases. This implies that the proposed method is particularly effective in scenarios with high SNR.

Table 4. 17: BER of proposed method and other scalable precoding techniques at L = 400 and N = 4, and K=100 with different SNR values.

Bit Error Rate of Precoding techniques based on SNR values (dB)					
S.No	SNR(dB)	LPMMSE	PRZF	PMMSE	Proposed
1	-15dB	0.44105	0.44105	0.43355	0.4212
2	-10dB	0.39681	0.3865	0.37444	0.34585
3	-5dB	0.29681	0.29363	0.28863	0.228025
4	0dB	0.20965	0.1856	0.178875	0.111213
5	5dB	0.166136	0.119138	0.071925	0.023812
6	10dB	0.14835	0.0851	0.014937	0.000412

Table 4.17 compares the performance of the proposed method and various centralized and distributed precoding techniques in terms of Bit Error Rate (BER). The table specifically focuses on the parameter values of L = 400, N = 4, and K = 100.

The analysis of Table 4.17 reveals that the proposed precoding method consistently performs better than LPMMSE, PRZF, and PMMSE techniques in terms of Bit Error Rate (BER). The BER values for the proposed method consistently indicate lower error rates, implying superior performance.

CHAPTER FIVE

5. CONCLUSION AND RECOMMENDATION

5.1. Conclusion

Dynamic clustering enables the cell-free network to intelligently group user equipment (UE) and access points (AP) based on channel conditions and traffic requirements. This clustering approach ensures efficient allocation of resources and promotes cooperative transmission, leading to the maximization of the system's overall performance. Generally, the dynamic clustering cooperation approach for scalable cell-free downlink operation shows great potential in optimizing resource allocation, reducing interference, improving spectral efficiency, and delivering reliable wireless communication. Its adaptability and scalability make it a promising solution for future wireless networks, ultimately enhancing performance and user experience. The spectral efficiency is a crucial metric that measures the amount of data that can be transmitted in the downlink direction per unit of bandwidth. By evaluating the sum spectral efficiency, which considers all UEs in the system, we can assess the overall efficiency and effectiveness of different precoding techniques. The proposed method consistently achieves the highest sum spectral efficiency per UE across different UE densities.

Overall, the analysis indicates that the proposed method offers enhanced overall downlink spectral efficiency per UE, making it a promising approach for maximizing data transmission rates and utilizing the available bandwidth efficiently. The performance gap between the proposed method and the other techniques widens as the the number of antenna within Aps and SNR values increases. This implies that the proposed method is particularly effective in scenarios with high SNR and higher number of antennas and UEs.

The gradient descent optimization technique is employed to progressively refine the MMSE precoding matrix, denoted as PMMSE. This is achieved by calculating the gradient of the mean squared error (MSE) with respect to the precoding matrix PMMSE, and then using this gradient information to iteratively update the precoding matrix. The goal of this approach is to minimize the MSE between the intended signal and the received signal, which ultimately results in enhanced performance for the downlink communication in massive MIMO systems.

5.2. Recommendation

Based on the potential and advantages of dynamic clustering cooperation for scalable cell-free downlink operation, here are some recommendations for future work:

Develop advanced algorithms to optimize dynamic clustering in cell-free networks, focusing on resource allocation, interference management, load balancing, and system capacity. Consider incorporating machine learning or artificial intelligence techniques. Investigate integration of dynamic clustering with other emerging technologies like mmWave communications, massive MIMO, or network slicing to enhance performance in cell-free downlink operations. Address security and privacy concerns in dynamic clustering. Develop robust authentication, encryption, and privacy-preserving mechanisms to protect user data and ensure communication integrity and confidentiality within clusters.

By pursuing these recommendations, researchers can advance the implementation of dynamic clustering for scalable cell-free downlink operation, leading to more efficient and reliable wireless networks.

REFERENCES

Abdallah, A., & Mansour, M. M. (2020). Efficient angle-domain processing for FDD-based cell-free massive MIMO systems. IEEE Transactions on Communications, 68(4), 2188-2203.

Björnson, E., & Sanguinetti, L. (2019a). Making cell-free massive MIMO competitive with MMSE processing and centralized implementation. IEEE Transactions on Wireless Communications, 19(1), 77-90.

Björnson, E., & Sanguinetti, L. (2019b). A new look at cell-free massive MIMO: Making it practical with dynamic cooperation. 2019 IEEE 30th annual international symposium on personal, Indoor and Mobile Radio Communications (PIMRC),

Björnson, E., & Sanguinetti, L. (2020). Scalable cell-free massive MIMO systems. IEEE Transactions on Communications, 68(7), 4247-4261.

Chen, S., Zhang, J., Björnson, E., Zhang, J., & Ai, B. (2020). Structured massive access for scalable cell-free massive MIMO systems. IEEE Journal on Selected Areas in Communications, 39(4), 1086-1100.

Demir, O. T., Björnson, E., & Sanguinetti, L. (2021). Cell-free massive MIMO with large-scale fading decoding and dynamic cooperation clustering. WSA 2021; 25th International ITG Workshop on Smart Antennas,

Ding, J., Nemati, M., Ranaweera, C., & Choi, J. (2020). IoT connectivity technologies and applications: A survey. IEEE Access, 8, 67646-67673.

Dong, Y., Zhang, Z., Liang, C., Yin, X., Wang, X., Zou, R., & Dai, X. (2018). A low-complexity precoding method based on the steepest descent algorithm for downlink massive MIMO systems. 2018 IEEE/CIC International Conference on Communications in China (ICCC),

Garg, N., Ge, H., & Ratnarajah, T. (2022). Generalized superimposed training scheme in IRS-assisted cell-free massive MIMO systems. IEEE Journal of Selected Topics in Signal Processing, 16(5), 1157-1171.

Hassan, B., Baig, S., & Aslam, S. (2023). On Scalability of FDD-Based Cell-Free Massive MIMO Framework. Sensors, 23(15), 6991.

Hoffmann, M., & Kryszkiewicz, P. (2024). Evaluation of User-Centric Cell-Free Massive Multiple-Input Multiple-Output Networks Considering Realistic Channels and Frontend Nonlinear Distortion. Applied Sciences, 14(5), 1684.

Interdonato, G., Buzzi, S., D'andrea, C., Venturino, L., D'elia, C., & Vendittelli, P. (2023). On the coexistence of eMBB and URLLC in multi-cell massive MIMO. IEEE Open Journal of the Communications Society.

Interdonato, G., Frenger, P., & Larsson, E. G. (2019). Scalability aspects of cell-free massive MIMO. ICC 2019-2019 IEEE International Conference on Communications (ICC),

Mai, T. C., Ngo, H. Q., & Duong, T. Q. (2020). Downlink spectral efficiency of cell-free massive MIMO systems with multi-antenna users. IEEE Transactions on Communications, 68(8), 4803-4815.

Marzetta, T. L., Larsson, E. G., & Hansen, T. B. (2020). Massive MIMO and beyond. In Information Theoretic Perspectives on 5G Systems and Beyond. Cambridge University Press.

Ngo, H. Q., Tran, L.-N., Duong, T. Q., Matthaiou, M., & Larsson, E. G. (2017). On the total energy efficiency of cell-free massive MIMO. IEEE Transactions on Green Communications and Networking, 2(1), 25-39.

Nguyen, H. V., Nguyen, V.-D., Dobre, O. A., Sharma, S. K., Chatzinotas, S., Ottersten, B., & Shin, O.-S. (2020). On the spectral and energy efficiencies of full-duplex cell-free massive MIMO. IEEE Journal on Selected Areas in Communications, 38(8), 1698-1718.

Özdogan, Ö., Björnson, E., & Zhang, J. (2019). Performance of cell-free massive MIMO with Rician fading and phase shifts. IEEE Transactions on Wireless Communications, 18(11), 5299-5315.

Papazafeiropoulos, A., Björnson, E., Kourtessis, P., Chatzinotas, S., & Senior, J. M. (2021). Scalable cell-free massive MIMO systems: Impact of hardware impairments. IEEE Transactions on Vehicular Technology, 70(10), 9701-9715.

Rahmani, M., Dehghani, M. J., Xiao, P., Bashar, M., & Debbah, M. (2022). Multi-agent reinforcement learning-based pilot assignment for cell-free massive MIMO systems. IEEE Access, 10, 120492-120502.

Ruan, Y., Chen, L., Zhou, X., Guo, G., & Chen, R. (2022). Hi-Loc: Hybrid indoor localization via enhanced 5G NR CSI. IEEE Transactions on Instrumentation and Measurement, 71, 1-15.

Sheela Rani, N., Vishnu Vardhan, D., Mamatha, G., Gunjan, V. K., & Shaik, F. (2022). Cell-Free Massive MIMO Versus Small Cells. International Conference on Information and Management Engineering, Sheikh, J. A., Haseena, H., & Mustafa, F. (2023). A New Dynamic Cooperation Cluster Empowered Cell-Free Massive MIMO Architecture Network for Future Networks.

Tuğfe Demir, Ö., Björnson, E., & Sanguinetti, L. (2021). Foundations of user-centric cell-free massive mimo. arXiv e-prints, arXiv: 2108.02541.

Xia, X., Zhu, P., Li, J., Wu, H., Wang, D., & Xin, Y. (2021). Joint optimization of spectral efficiency for cell-free massive MIMO with network-assisted full duplexing. Science China Information Sciences, 64, 1-16.

Ye, F., Li, J., Zhu, P., Wang, D., Wu, H., & You, X. (2022). Spectral efficiency analysis of cell-free distributed massive MIMO systems with imperfect covariance matrix. IEEE Systems Journal, 16(4), 5402-5412.

Zaher, M., Demir, Ö. T., Björnson, E., & Petrova, M. (2022). Learning-based downlink power allocation in cell-free massive MIMO systems. IEEE Transactions on Wireless Communications, 22(1), 174-188.

Zhang, H., Li, H., Wang, X., Cheng, W., Dong, L., & Shi, G. (2024). Scalable Cache-Aided Cell-Free Massive MIMO Systems. IEEE Wireless Communications Letters.

Zhang, H., Su, R., Zhu, Y., Long, K., & Karagiannidis, G. K. (2022). User-centric cell-free massive MIMO system for indoor industrial networks. IEEE Transactions on Communications, 70(11), 7644-7655.

Zhang, J., Chen, S., Lin, Y., Zheng, J., Ai, B., & Hanzo, L. (2019). Cell-free massive MIMO: A new next-generation paradigm. IEEE Access, 7, 99878-99888.

Zhang, X., Liang, T., An, K., Yang, H., & Niu, C. (2022). Secure transmission in RIS-assisted cell-free massive MIMO system with low resolution ADCs/DACs. 2022 IEEE Wireless Communications and Networking Conference (WCNC),

Zhang, X., Qiao, X., An, K., Deng, J., Liang, T., & Wang, X. (2022). Reconfigurable Intelligent Surface-Aided Cell-Free Massive MIMO with Low-Resolution ADCs: Secrecy Performance Analysis and Optimization. Wireless Communications and Mobile Computing, 2022, 8462350. https://doi.org/10.1155/2022/8462350

Zheng, J., Zhang, J., Du, H., Niyato, D., Ai, B., Debbah, M., & Letaief, K. B. (2024). Mobile cell-free massive MIMO: Challenges, solutions, and future directions. IEEE Wireless Communications.

Zheng, J., Zhao, Z., Zhang, J., Cheng, J., & Leung, V. C. (2022). Performance analysis of cell-free massive MIMO systems with asynchronous reception. 2022 IEEE Globecom Workshops (GC Wkshps),